THE PRODUCTION OF THYMOQUINONE FROM THYMOL AND CARVACROL BY USING ZEOLITE CATALYSTS

A Thesis Submitted to
The Graduate School of Engineering and Sciences of
İzmir Institute of Technology
in Partial Fulfillment of the Requirements for the Degree of

MASTER OF SCIENCE

in Chemical Engineering

by
Alev GÜNEŞ

July 2005
İZMİR

We approve the thesis of **Alev GÜNEŞ**

Date of Signature

..... **22 July 2005**
Asst. Prof. Dr. Oğuz BAYRAKTAR
Supervisor
Department of Chemical Engineering
İzmir Institute of Technology

..... **22 July 2005**

Assoc. Prof. Dr. Selahattin YILMAZ
Co-Supervisor
Department of Chemical Engineering
İzmir Institute of Technology

..... **22 July 2005**

Asst. Prof. Dr. Fehime ÖZKAN
Department of Chemical Engineering
İzmir Institute of Technology

..... **22 July 2005**
Asst. Prof. Dr. Ali ÇAĞIR
Department of Chemistry
İzmir Institute of Technology

..... **22 July 2005**
Prof. Dr. Devrim BALKÖSE
Head of Department
İzmir Institute of Technology

.....
Assoc. Prof. Dr. Semahat ÖZDEMİR
Head of Graduate School

ACKNOWLEDGEMENTS

I would like to acknowledge the people who have helped to make this work possible. My sincere gratitude is first for my thesis advisor Assist. Prof. Oğuz BAYRAKTAR for his consistent and thoughtful advice, continuous encouragement and help during the course of this work. I am also grateful to my other advisor Assoc. Prof. Selahattin YILMAZ for his valuable comments and recommendations.

I also wish to thank to personnel of IZTECH Centre for Material Research for their help during my material characterization studies.

I would like to appreciate deeply to my roommates, Bahar BOZKURT, Gözde GENÇ for their friendships, supports and encouragements.

I am grateful to my friends for assisting me with my research and offering advice and discussion. I also present my deepest thanks to Burç YERKESİKLİ because of not only his friendship but also his kind of efforts and endless support.

Finally, I would like to express my heartfelt gratitude to my parents, Neşe and Mehmet Ali GÜNEŞ and brother, Batuhan GÜNEŞ for their continuous support and encouragement, which enabled me to overcome difficulties.

ABSTRACT

In this thesis study, by using general flexible ligand method, Cr(III), Fe(III), Bi(III), Ni(II) and Zn(II) complexes of N,N´-bis(salicylidene)propane-1,3-diamine (H_2salpn) encapsulated in NaY-zeolite were prepared. All catalyst were characterized by Fourier transform infrared (FT-IR), X-ray diffraction (XRD) and Scanning electron microscopy (SEM) analyses to confirm the complex encapsulation.

Activities of all prepared catalysts for the decomposition of hydrogen peroxide and oxidation of carvacrol were tested. Leaching test or heterogeneity test was also performed. The performances of all catalysts were compared based on the leaching test results and carvacrol conversion. Thymohydroquinone and benzoquinones were observed as by-products at high conversions of carvacrol. No product was formed in the absence of a catalyst. Fe(salpn)-NaY catalyst has shown the highest carvacrol conversion of 27.6% with a yield of 22.0% which was followed by Cr(salpn)-NaY catalyst with 23.5% carvacrol conversion with a yield of 17.6%. Other catalysts have shown relatively lower performances in terms of carvacrol conversion and leaching. The Cr(salpn)-NaY catalyst was found to be a more efficient catalyst than others based on leaching and activity tests. Selected catalyst was extra characterized by Brunauer Emmett and Teller (BET) and Thermal gravimetric (TGA) analyses. With selected catalyst Cr (salpn)-NaY, temperature, catalyst amount, reactant carvacrol to hydrogen peroxide molar ratio effects were investigated in carvacrol oxidation reactions. Increasing the temperature from 40 to 60 ºC caused the increment of thymoquinone yield from 6.2 to 16.0%. In addition to that the yield of thymoquinone was increased from 7.4 to 20.7% by increasing catalyst amount from 0.05 to 0.2 g. And also thymoquione yield was increased from 3.7 to 23.0% by decreasing carvacrol to hydrogen peroxide molar ratio from 1 to 3. Moreover, Cr (salpn)-Y catalyst was also tested in thymol and essential oil oxidation reactions.

ÖZET

Bu tezde, genel esnek ligand metodu kullanılarak Na-Y zeoliti içerisine enkapsüle edilmiş N.N'-bis (salicylidene)propane-1,3-diamine (H_2salpn) in Cr (III), Fe(III), Bi(III), Ni(II) ve Zn(II) kompleksleri hazırlanmıştır. Hazırlanan bu katalizörler Fourier transformu kızılötesi (FT-IR), X-ışın kırınımı (XRD) ile taramalı elektron mikroskobu (SEM) ile karakterize edilmiştir.

Hazırlanan tüm katalizörlerin aktiviteleri, hidrojen peroksit bozunmasında ve karvakrol ün oksidasyonu reaksiyonlarında test edilmiştir. Katalizörlerdeki metal komplekslerin sıvı faza geçişi (hetorejenlik) testleri gerçekleştirilmiştir. Katalizör aktiviteleri, karvakrol dönüşümü ve aktif metallerin sıvı faza geçmesi kavramları bakımından karşılaştırılmıştır. Yüksek karvakrol dönüşümlerinde thymoquinone ile yan ürün olarak thymohydroquione ve benzoquinone elde edilmiştir. Katalizör yokluğunda ürün elde edilmemektedir. Fe(salpn)-NaY katalizörü % 27.6 ile en yüksek karvakrol dönüşümü gösterirken, bunu % 23.5 karvakrol dönüşümü ile Cr(salpn)-NaY katalizörü izlemiştir. Diğer katalizörler, karvakrol dönüşümü ve aktif metallerin sıvı faza geçmesi kavramları bakımından daha düşük performans göstermişlerdir. Cr(salpn)-NaY katalizörü aktif metallerin sıvı faza geçmesi ile aktiflik deneylerine dayalı olarak diğerlerine göre daha etkin bir katalizör olarak bulunmuştur. Seçilen Cr (salpn)-NaY katalizörü ekstra olarak BET ve TGA analizleri ile karakterize edilmiştir. Bu katalizörle, sıcaklığın, katalizör miktarının, karvakrolün hidrojen peroksite molar oranının; karvakrol oksidasyonu reaksiyonlarına etkileri incelenmiştir. Sıcaklığın 40 ºC den 60 ºC yükseltilmesiyle, thymoquinone oluşumunun % 6.2 den % 16 ya arttığı gözlenmiştir. Buna ek olarak katalizör miktarının 0.05 gr dan 0.2 gr'a artışıyla thymoquinone oluşumunda % 7.4 den % 20.7 ye artış gözlenmiştir. Ayrıca karvakrolün hidrojen peroksite molar oranının 3 ten 1'e inişiyle (hidrojen peroksit miktarının artışıyla), thymoquinone oluşumu %3.7 den %27 ye artmıştır. Buna ek olarak, Cr (salpn)-NaY katalizörü thymol ve kekik yağı oksidasyonunda test edilmiştir.

TABLE OF CONTENTS

LIST OF FIGURES

LIST OF TABLES

Table **Page**

CHAPTER 1

INTRODUCTION

The development of efficient catalysts for the oxidation of organic compounds in environmental friendly conditions is an active field of research. Although homogeneous metal complex catalysts exhibit good activity and selectivity, heterogenization of homogeneous metal-complex catalysts by encapsulating them inside the zeolite possesses the advantages of both homogeneous and heterogeneous counterpart like easy separation, rigidity, site isolation effect (Maurya et al. 2002a). Site isolation of redox active metal centers in zeolite cages can afford the catalysts higher activity by separating redox metal centers in inorganic matrix (Sheldon et al. 1998). Heterogeneous catalysts can be prepared by using ship in a bottle method (Arends et al. 2001). This method involves assembling a metal complex in intrazeolite space such that the complex, once formed, is too large to diffuse out. If leaching of zeolite-encapsulated metal complexes does not occur under the reaction conditions, catalyst is said to be completely heterogeneous. Recently, metal complexes of porphyrins, salen, salpn and phthalocyanines have been encapsulated into zeolitic matrix for the development of efficient oxidation catalysts (Skrobot et al. 2003, Nakagaki et al. 2000, Maurya et al. 2002, Shevade et al. 1999).However, the most important question of metal leaching was not considered in these studies.

Chemical transformation of abundant and cheap products into novel and more valuable compounds can be achieved by liquid-phase oxidation reactions using hydrogen peroxide as clean oxidant (Martin et al. 1999). Hydrogen peroxide is one of the preferred oxidants because it is easy to handle and its reaction produces only water as by-product (Arends et al. 2001). Catalytic oxidation of aromatic monoterpenes with hydrogen peroxide is a reaction of industrial importance (Monteiro et al. 2004). Carvacrol is the example of p-menthane type aromatic monoterpene, which can be found in the essential oils of several aromatic plants. Carvacrol and its geometrical isomers thymol can be oxidized to thymoquinone, which has a commercial value considerably higher than its precursor's thymol and carvacrol. Thymoquinone has antitumor and hepatoprotective activity (Badary et al. 1999). Since the natural resources

of thymoquinone are limited only to certain plant resources such as *Nigella Sativa, Callitris articulata* there is a growing interest for its production. It is well established that the chemical transformation of abundant and cheap natural products can make available other more valuable products.

Essential oil rich in carvacrol and thymol were easily oxidized to oil containing thymoquinone as the main component in the presence of Fe(III) porphyrin and phtylocyanine complexes (Milos et al. 2001). The carvacrol oxidation with hydrogen peroxide was also studied using Mn(III) porphyrin complexes and keggin-type tungstoborates (Martin et al. 1999, Santos et al. 2003). Oxidation of carvacrol yielded a mixture of benzoquinones containing a small amount of thymoquinone for keggin-type tungstoborates whereas for Mn(III) porphyrin complexes oxidation of carvacrol selectively yielded thymoquinone. Thymoquinone can be obtained in carvacrol oxidation reactions catalyzed by zeolite encapsulated metal complexes. Oxidation of carvacrol and thymol in the presence of Y-zeolite-entrapped porphyrin complexes was studied by Skrobot et al. (2003). The oxidation of carvacrol (<25% conversion) and thymol (<18% conversion) gave thymoquinone with 100% selectivity. However, leaching of the porphyrin complex from the zeolitic matrix occurred in the presence of H_2O_2.

In this thesis study, zeolite encapsulated metal (Fe, Cr, Zn, Ni, Bi) complexes were prepared by general flexible ligand method as described in the literature (Maurya et al. 2002). H_2salpn was used as a flexible ligand. Prepared catalysts were characterized by using FTIR, XRD, BET and TGA to confirm the metal complex encapsulation. To our knowledge no previous studies on the oxidation of carvacrol in the presence of metal salpn complexes have been studied before. Activities of the catalysts for the decomposition of hydrogen peroxide and oxidation of carvacrol to form thymoquinone were tested. Leaching of active metal center into the reaction medium is the most important problem for the zeolite-encapsulated metal complexes. Catalyst screening process was performed according to leaching test results and catalytic oxidation activities. With selected catalyst, some parameters effects on carvacrol oxidation reaction were investigated. And also, application of this catalyst on the thymol and essential oil oxidation reactions were studied.

CHAPTER 2

CATALYSTS AND ZEOLITE PROPERTIES

2.1. Definition of Catalyst and Zeolite

Catalytic phenomena affect virtually all aspect of our life. They are important in the processing of the foods and the production of the medicine, in the refining of the petroleum, manufacture of plastics and the production of many different chemicals (Sinfelt 2002).

A catalyst is a substance that increases the rate at which chemical reactions approaches equilibrium without itself becoming permanently involved in the reaction. The catalyst accelerates the kinetics of the reaction toward the thermodynamic completion by introducing a less difficult path for molecules to follow (Satterfield 1991). Catalysts have three types of components: active components, a support or carrier and promoters. Active components are responsible for the principle chemical reaction. In some cases a catalyst consists of minute particles of an active material dispersed over a less active substance called a support. The promoter is a substance that, when added in relatively small amounts in the preparation of catalysts, imparts better activity and selectivity (Richardson 1989).

Catalysts are often classified as biological catalysts (enzymes), homogeneous and heterogeneous. In biological catalysts systems, the most of the reactions occur in living organisms. These types of biochemical reactions are catalyzed by molecules called enzymes (Sinfelt 2002).

In homogeneous catalysts systems, the catalyst is in the same phase as the reactants and products. Acid and base catalysts are the most important types of homogeneous catalysts in liquid solution. Advantages of homogeneous catalysis on an industrial scale are high selectivity and ease of heat dissipation from exothermic reactions. However, separation is a major problem for these reactions.

In heterogeneous catalysts systems, the reactants and catalyst exist in different phases. Running a reaction under heterogeneous catalytic conditions has several

advantages compared to homogeneous catalysts such as regeneration, long life, recycling, easy separation (Richardson 1989).

Zeolites have been playing an important role in heterogeneous catalysts. In many industrial processes such as petrochemistry and the manufacture of organic chemicals are carried out using zeolite catalysts. Altogether, zeolite catalysts have become a most important sub-field of heterogeneous catalysts (Weitkamp 1999). So the next section involves the usage of zeolite as heterogeneous catalyst.

2.2. Zeolite as Heterogeneous Catalyst

Zeolites are formed in nature or synthesized. They are porous, crystalline, hydrated aluminosilicates of group IA and group IIA elements such as sodium, potassium, magnesium, calcium, strontium and barium (Richardson 1989).

In 1976, the Swedish mineralogist Cronstedt discovered that a particular type of mineral lost water upon heating. He called this mineral a "zeolite", from the Greek "zeo" to boil, and "lithos" stone, because many zeolite appear to boil when heated (Richardson 1989).

Synthetic zeolites give currently massive efforts in trying to synthesize new kinds of zeolite type materials (Weitkamp 1999). This research partly involves a study of preparing heterogeneous catalysts with synthesised sodium zeolite Y. This zeolite has a faujasite structure, with Na^+ ions inside the framework on various sites.

Many reactions showed the advantages of the zeolites compared to the conventional liquid acids in terms of easy separation, control of the production, shape selectivity effects and the possibility of the regeneration. During the last two decades an increasing number of publications have appeared reporting the use of zeolites as solid catalysts for liquid phase reactions for the production of fine chemicals (Maurya et al. 2002a).

2.3. Structural Features of Zeolite

Zeolites comprise a three-dimensional crystal network of Si and Al atoms, which are present in the form of SiO_4 and $(AlO_4)^-$ tetrahedral. Tetrahedrals join together in

shared oxygen atoms with various regular arrangements, to form hundreds of different three-dimensional crystal frameworks (Kaduk et al. 1995).

The framework structure encloses cavities containing pores of molecular dimensions. Their frameworks are made up of 4-connected networks of atoms. One way of thinking about this is in terms of tetrahedra, with a silicon atom in the middle and oxygen atoms at the corners. These tetrahedra can then link together by their corners as seen in Figure 2.1. Zeolite Y has a faujasite type framework structure, with three different cavities or cages which are the large supercage, the sodalite cage and the double 6-ring.

The structural formula of a zeolite for a crystallographic unit cell is:

$M_{x/n}((AlO_2)_x(SiO_2)_y).wH_2O$

Where M is the cation of valance of n, w is the number of water molecules. The ratio y/x (Si/Al ratio) usually has values of 1-5 depending upon the structure. The sum (x+y) is total number of tetrahedral in the unit cell (Breck 1974).

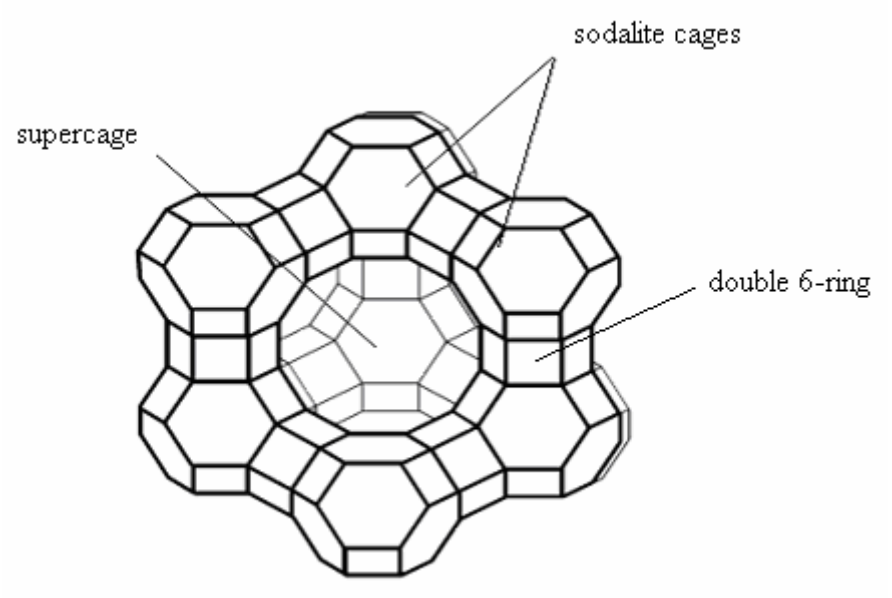

Figure 2.1. Framework structure of zeolite Y

(Source: Kaduk et al. 1995)

The replacement of SiO_4 tetrahedra by the $(AlO_4)^-$ tetrahedral in the zeolite framework causes excess negative charge. Cations are needed to neutralize. Compensation of negative charge by associated cations such as; H^+, Na^+, K^+, Ca^{+2},

NH_4^{+2} generates the acid sides. Catalytic activity of the zeolites is attributed to the presence of these acidic sites.

The most commonly encountered faujasites are zeolites X (higher Al) and zeolite Y (lower Al). Zeolite Y is the most important catalytic zeolite, and is generally synthesized in the Na form (Richardson 1989).

There are 70 known different kinds of building arrangements, each resulting in a distinct structure. Some of these occur as natural minerals; some are synthetic. Catalytically important zeolites are listed in Table 2.1 (Sen et al. 1999, Richardson 1989).

Table 2.1. Catalytic zeolites
(Source: Richardson 1989)

Zeolite	Pore type	Dimensions(Å)
Faujasite, X, Y	interconnected spheres	4.1 Å diameter pore 11.4 Å diameter cavity
Modernite	interconnected channels	6.5x7.0 Å channels 2.6x5.7 Å channels
Zeolite beta	interconnected channels	7.6x6.4 Å channels 5.5x5.5 Å channels
ZSM –5	interconnected channels	5.3x6 Å channels 5.1x5.5 Å channels
Zeolite A	interconnected spheres	4.1 Å diameter pore 11.4 Å diameter cavity

2.4 Properties of Zeolite

A large-pore zeolite such as zeolite Y, whose structure consists of almost spherical 13 Å supercages interconnected tetrahedrally through smaller apertures of 7.4 Å in diameter. This is limited regarding the size of guest molecules by the space available in these cavities (Hoelderich et al. 2000).

Zeolite properties can be changed with modification of cation exchange, impregnation. These techniques are used to introduce metal into zeolites. Impregnation

is the simplest and most direct method. Pores are filled with a solution of metal salt of sufficient concentration to give correct loading. Ion exchange is the reversible interchange of ions between a solid and a liquid. There is no permanent change in the structure of the solid, which is the ion exchange material. Usually, contacting a zeolite with a salt solution of different cation performs ion exchange; one type of cation is replaced with other.

The ion exchange process:

$$z_A B^{zB}_{(z)} + z_B A^{zA}_{(s)} + \rightleftharpoons z_A B^{zB}_{(s)} + z_B A^{zA}_{(z)}$$

Where z_A and z_B are the charges of the exchange cation A and B and the subscript z and s refer to the zeolite and solution, respectively.

A widely recognized modification of catalyst is to replace the Na^+ ions with other metal ions and then reduce them in situ so that the metal atoms are deposited within the framework. The resultant material displays the properties associated with a supported metal catalyst. Ion exchanged cation can induce new catalytic features in many reactions especially in liquid phase reactions, by their different size and chemical structure (Sheldon et al. 1998).

2.5 Design of Stable Heterogeneous Catalysts

Liquid phase oxidation is widely used in bulk chemical manufacture. It is becoming increasingly important in the synthesis of fine chemical (Arends et al. 2001). Catalytic oxidations in the liquid phase generally employ soluble metal salts or complexes in combination with clean, inexpensive oxidants such as O_2, H_2O_2, or RO_2H. Heterogeneous catalysts are widely used in liquid phase oxidation reactions because of their advantages.

For heterogeneous catalysts; incorporation of the redox metal centre into the surface of an oxide support is the conventional methods for the immobilizing metal catalyst. Such as heterogeneous Ti^{IV}/SiO_2 catalysts which is used for the epoxidation of the propylene (Arends et al. 2001; Sheldon et al. 1998).

Another approach to design stable solid catalysts is confinement of redox metal ions or complexes into the framework or cavities of zeolites, redox molecular sieves. Unlike conventional supported catalysts; they have a regular microenvironment with

homogeneous internal structures which consisting of uniform, well-defined cavities and channels of molecular dimensions. Confinement of the redox active site in channels or cavities can endow the catalyst with over higher activity than the conventional catalyst (Arends et al. 2001, Sheldon et al. 1998).

Confinement of the redox active sites in channels provides site-isolation of active metal ions or complexes in inorganic matrices. This prevents their dimerization or oligomerization to less reactive species. Site-isolation of different redox metal centres in inorganic matrices can afford oxidation catalysts with higher activities (Arends et al. 2001).

A major disadvantage of this approach is the mobility of the metal ion (leaching into solution). This generally involves solvolysis of M-O-surface bonds by reaction with polar solvents. Since the products of oxidation reactions are usually polar molecules, leaching will be a problem. And also the usage of mesoporous molecular sieves, such as USY zeolites and MCM-41 suffers from leaching as an effect of the pores being open to the external surface. The synthetic utility of solid catalysts stands or falls with their stability towards leaching. (Arends et al. 2001, Sheldon et al. 1998, Kaduk et al. 1995).

Various methods as described in Figure 2.2 can be employed for immobilizing redox active elements in a solid inorganic matrix. These are; (a) substitution of metals in framework of silicalites, zeolites, aluminaphosphate (AlPOs) and silica-aluminaphosphates (SAPOs) (b,c) grafting and tethering of metal complexes to the internal surface of the molecular sieves (d) encapsulation of metal complexes in intrazeolite space, ship in a bottle catalyst as seen in Figure 2.2.

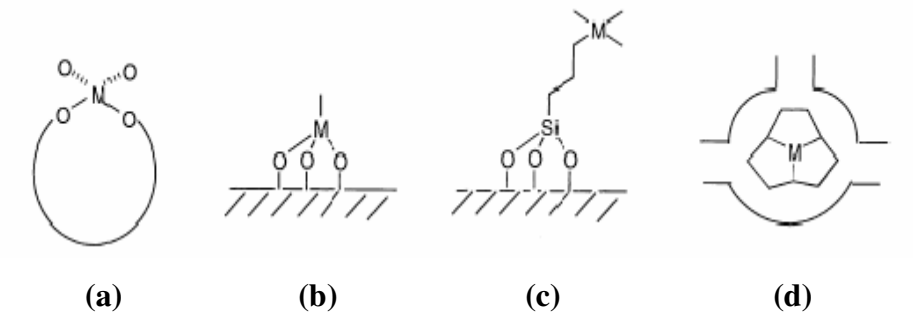

Figure 2.2. Strategies for heterogenization of metal centre (M) (a) Framework substituted (b) Grafted (c) Tethered (d) Ship in a bottle
(Source: Arends et al. 2001)

Metal ions can be isomorphously substituted in framework positions of moleculer sieves such as zeolites, silicalites, aluminaphosphates (APOs), silica-aluminaphosphates (SAPOs), via hydrothermal or post synthesis modification. Amorphous mixed oxides can be prepared by grafting of metal compound on the surface of, e.g. silica. Metal complexes can be tethered to the surface of solid, e.g. silica with ligand. The major disadvantages of substitution, grafting and tethering is the mobility of the metal ion. The final approach is to encapsulate transition metal complexes in a solid inorganic matrix (ship in a bottle concept). It involves the entrapment of complex in zeolite supercages (Arends et al. 2001). Transition metals react with a variety of molecules or groups, called ligands to form metal complexes. These transition metal complexes act as catalyst (Solomons 1988).

CHAPTER 3

TRANSITION METALS AND COORDINATION CHEMISTRY

3.1. Definition and Physical Properties of Transition Metals

The transition metals constitute groups 3 through 12 of the periodic table. They're the elements which have partially filled d-shells and Zn, Cd and Hg are included even though their d-shells are entirely filled. The first row transition metals have the electronic configuration [Ar] $3d^n$ $4s^m$ where n is between1-10 and m is between1-2. The second row has the configuration [Kr] 4d 5s, and the third row have the configuration [Xe] 5d 6s (Solomons 1988).

IIIB, IVB, VB, VIB, VIIB, VIII, IB, IIB elements of the periodic table are the transition metals that are the most concern. As with all metals, the transition elements are both ductile and malleable, and conduct electricity and heat. Similarities occur within a period as well as within a group due to last electrons (Solomons 1988).

The elements in the periodic table as shown in Figure 3.1 are often divided into four categories: (1) main group elements, (2) transition metals, (3) lanthanides, and (4) actinides. The main group elements include the active metals in the two columns on the extreme left of the periodic table and the metals, semimetals, and nonmetals in the six columns on the far right. The transition metals are the metallic elements that serve as a bridge, or transition, between the two sides of the table. The lanthanides and the actinides (f block elements) at the bottom of the table are sometimes known as the inner transition metals because they have atomic numbers that fall between the first and second elements in the last two rows of the transition metals. f-block elements are not traditionally treated as transition elements since f electrons do not affect bonding. Transition metals are more electronegative than the main group metals; therefore they are more likely to form covalent compounds (Morrison 1992).

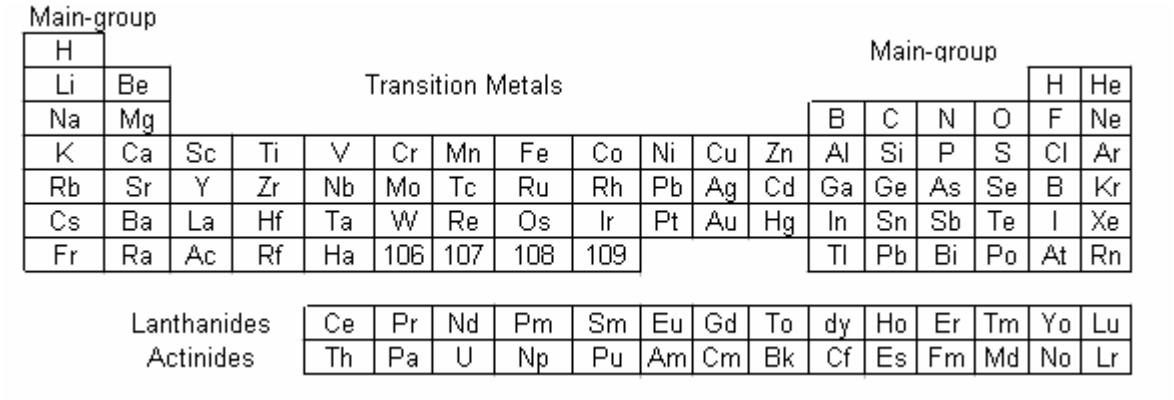

Figure 3.1. Position of transition metals in the periodic table.
(Source: Solomons 1988)

Another difference between the main group metals and transition metals can be seen in the formulas of the compounds they form. The main group metals tend to form salts (such as NaCl, Mg_3N_2, and CaS) in which there are just enough negative ions to balance the charge on the positive ions. The transition metals form similar compounds (e.g., $FeCl_3$, HgI_2, or $Cd(OH)_2$), but they are more likely than main group metals to form complexes, such as the $FeCl_4^-$, HgI_4^{2-}, and $Cd(OH)_4^{2-}$ ions, that have an excess number of negative ions. A third difference between main group and transition-metal ions is the ease with which they form stable compounds with neutral molecules, such as water or ammonia (Morrison 1992).

3.2. Electronic Configuration

The electronic configuration of the atoms of the first row transition elements are basically the same. It can be seen in the Table 3.1, there is a gradual filling of the 3d orbitals across the series starting from scandium. This filling is not regular, since for chromium and copper the population of 3d orbitals increase by the acquisition of an electron from the 4s shell. For chromium, both the 3d and 4s orbitals are occupied, but neither is completely filled in preference to the other. This suggests that the energies of the 3d and 4s orbitals are relatively close for atoms in this row. In copper, the 3d level is full, but only one electron occupies the 4s orbital. This suggests that in copper the 3d orbital energy is lower than the 4s orbital. Thus the 3d orbital energy has passed from higher to lower as we move across the period from potassium to zinc. However, the whole question of preference of an atom to adopt a particular electronic configuration is

not determined by orbital energy alone. In chromium it can be shown that the 4s orbital energy is still below the 3d which suggests a configuration [Ar] $3d^4 4s^2$. Due to the effect of electronic repulsion between the outer electrons the actual configuration becomes [Ar] $3d^5 4s^1$ where all the electrons in the outer orbitals are unpaired. The interesting thing about transition metals is the electrons they use to combine with other elements (valence electrons) are present in more than one shell. This is the reason why they often exhibit several common oxidation states. The elements in this group can have different oxidation states which makes them useful as catalyst.

Cr has only one electron in its 4s sub-shells because the other electron is used to make a half full 3d sub-shell which is more stable. The same argument goes for Cu, which makes a full 3d sub-shell. When the transition metals become ions they lose their 4s electrons first. Fe for example loses 3 electrons to become a Fe^{3+} ion. It will therefore lose 2 4s electrons and one 3d electron.The final configuration of the metal ion is stabilized if the electron configuration includes either half-full or full orbitals. The electrons may be shuffled between the s and d orbitals to maintain the most stable form.

The difference in energy between the second and third shells is less than between the first and second. By the time the fourth shell is reached, there is, in fact an overlap between the third and fourth shells. In other words, from scandium onwards, the orbitals of highest energy in the third shell (the 3d orbital) have higher energy than those of the lowest energy in the fourth shell (the 4s orbital). Hence, when writing the electronic configurations of these ‘d’ block elements we fill the 4s then the 3d orbitals. Exceptions do occur for Cr [Ar] $4s^1 3d^5$ and Cu [Ar] $4s^1 3d^{10}$.This can be explained by the extra stability offered by full and half-filled ‘d’ orbitals.

Table 3.1. Electronic Configuration of the free atoms of the first row transition elements (Source: Anthony 1999)

Potassium	K	(Ar) $4s^1$	K^+	(Ar)
Calcium	Ca	(Ar) $4s^2$	Ca^{2+}	(Ar)
Scandium	Sc	(Ar) $3d^1 4s^2$	Sc^{3+}	(Ar)
Titanium	Ti	(Ar) $3d^2 4s^2$	Ti^{4+}	(Ar)
Vanadium	V	(Ar) $3d^3 4s^2$	V^{3+}	(Ar) $3d^2$
Chromium	Cr	(Ar) $3d^5 4s^1$	Cr^{3+}	(Ar) $3d^3$
Manganese	Mn	(Ar) $3d^5 4s^2$	Mn^{2+}	(Ar) $3d^5$
Iron	Fe	(Ar) $3d^6 4s^2$	Fe^{2+}	(Ar) $3d^6$
			Fe^{3+}	(Ar) $3d^5$
Cobalt	Co	(Ar) $3d^7 4s^2$	Co^{2+}	(Ar) $3d^7$
Nickel	Ni	(Ar) $3d^8 4s^2$	Ni^{2+}	(Ar) $3d^8$
Copper	Cu	(Ar) $3d^{10} 4s^1$	Cu^+	(Ar) $3d^{10}$
			Cu^{2+}	(Ar) $3d^9$
Zinc	Zn	(Ar) $3d^{10} 4s^2$	Zn^{2+}	(Ar) $3d^{10}$

3.3. Oxidation State and Coordination Number

Transition metals have two types of valence (combining abilities); primary valence (oxidation state) is the ability to form ionic bonds with oppositely charged ions and secondary valence (coordination number).

3.3.1. Oxidation State

The transition metals show a formidable number of oxidation states. The reason for exhibiting such a variety of oxidation states is the closeness of 3d and 4s energy states. Table 3.2 summarizes known oxidation numbers of the first row transition elements. The most prevalent oxidation numbers are shown in bold. The oxidation number zero usually assigned to elemental state has been omitted from the Table.

Table 3.2. Known oxidation numbers of first row transition elements.
(Source: Anthony 1999)

Sc			**+3**				
Ti	+1	**+2**	**+3**	**+4**			
V	+1	**+2**	**+3**	**+4**	**+5**		
Cr	+1	**+2**	**+3**	+4	+5	**+6**	
Mn	+1	**+2**	**+3**	**+4**	+5	**+6**	**+7**
Fe	+1	**+2**	**+3**	+4	+5	+6	
Co	+1	**+2**	**+3**	+4	+5		
Ni	+1	**+2**	+3	+4			
Cu	**+1**	**+2**	+3				
Zn		**+2**					

There is an increase in the number of oxidation states from Sc to Mn. All seven oxidation states are exhibited by Mn. The formal oxidation number of +7 represents the formal loss of all seven electrons from 3d and 4s orbitals. In fact all of the elements in the series can utilize all the electrons in their 3d and 4s orbital. There is a decrease in the number of oxidation states from Mn to Zn. This is because the pairing of d-electrons occurs after Mn which in turn decreases the number of available unpaired electrons and hence, the number of oxidation states.

The stability of higher oxidation states decreases in moving from Sc to Zn. Mn(VII) and Fe(VI) are powerful oxidizing agents. The relative stability of +2 state with respect to higher oxidation states, particularly +3 state increases in moving from

left to right. This is justifiable since it will be increasingly difficult to remove the third electron from the d orbital. The lower oxidation states are usually found in ionic compounds and higher oxidation states tend to be involved in covalent compounds (Solomons 1988).

3.3.2. Coordination Number

Coordination number is the ability to bind to Lewis bases (ligands) to form coordination complex ions. In other words, coordination complexes are species in which a central metal is attached to ligand by coordinate covalent bonds. The central metal is a Lewis acid (electropositive). A Ligand is a Lewis base (electronegative). The total number of metal-ligand bonds is called the coordination number. Coordination number varies from two to eight and it depends on the size, charge, and electron configuration of the transition metal. Many metals show more than one coordination number (Solomons 1988).

Within a ligand, the metal ion is directly bonded to the donor atom. A coordinate covalent bond is a covalent bond in which one atom (i.e., the donor atom) supplies both electrons. This type of bonding is different from a normal covalent bond in which each atom supplies one electron. If the coordination complex carries a net charge, the complex is called a complex ion. Compounds that contain a coordination complex are called coordination compounds (Brunel et al. 1998).

3.4. Types of Ligands

Ligands are classified as monodentate, bidantate, polydentate ligands. Monodentate ligands bond using the electron pairs of a single atom. Bidentate ligands bond using the electron pairs of two atoms. Polydentate ligands bond using the electron pairs of many atoms. This group includes bidentate. Polydentate ligands are also known as chelating agent (Keim et al. 2002).

Monodentate (one tooth) ligand can only form one bond with the metal ion such as H_2O, CN^-, NH_3, NO_2^-, SCN^-, OH^-, Cl^-, etc. in Figure 3.2. Bidentate ligand can form two bonds to a metal such as Ethylenediamine, (H_2N-CH_2- CH_2-NH_2), oxalate in Figure 3.3. Polydentate ligands (chelating ligands) such as EDTA(ethylenediaminetetraacetate)

it surrounds the metal, forms very stable complex ions (Arends et al. 2001) as seen in Figure 3.4.

Any ion or molecule with a pair of nonbonding electrons can be a ligand. Many ligands are described as monodentate (literally, "one-toothed") because they "bite" the metal in only one place. Typical monodentate ligands are given in the figure below (Figgis 1966, Keim et al. 2002).

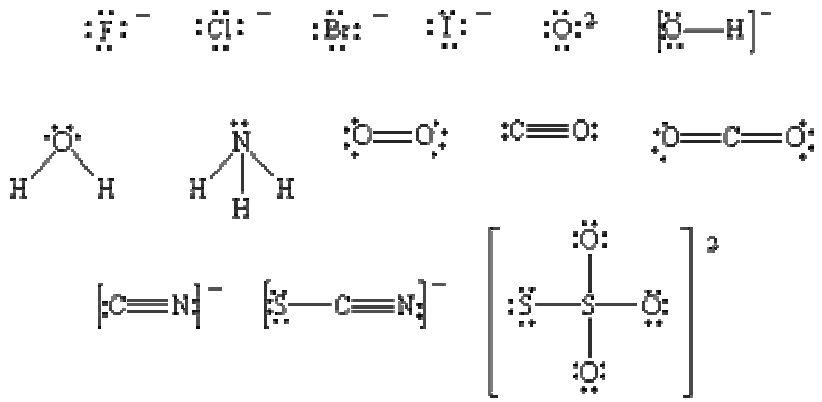

Figure 3.2. Typical monodentate ligands.
(Source: Keim et al. 2002)

Other ligands can attach to the metal more than one place. Ethylenediamine (en) is a typical bidentate ligand.

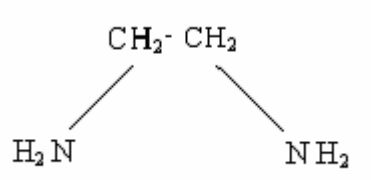

Figure 3.3. Bidentate ligand, ethylenediamine.
(Source: Keim et al. 2002)

Each end of this molecule contains a pair of nonbonding electrons that can form a covalent bond to a metal ion. Ethylenediamine is also an example of a chelating ligand. The term chelate comes from a Greek stem meaning "claw." It is used to describe ligands that can grab the metal in two or more places, the way a claw would. Linking ethylene- diamine fragments gives tridentate ligands and tetradentate ligands,

such as diethylenetriamine (dien) and triethylenetetramine (trien). Adding four -$CH_2CO_2^-$ groups to an ethylenediamine framework gives a hexadentate ligand, which can single-handedly satisfy the secondary valence of a transition-metal ion (Figgis 1966).

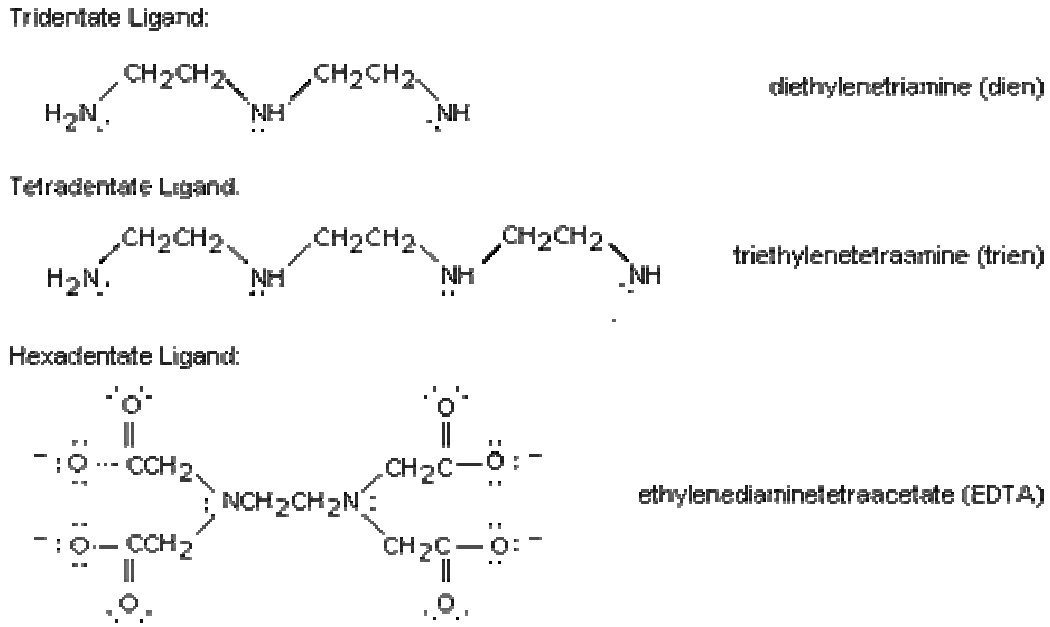

Figure 3.4. Typical polydentate ligands
(Source: Keim et al. 2002)

In the catalyst synthesis, the encapsulation of metal complexes into the zeolites method is known as a ship in a bottle procedure. Encapsulation of metal complexes is occurred in the super cages of the zeolite. Ship in a bottle approach involving the entrapments of a bulky complex in a zeolite cage, has been widely used to immobilize metal complexes of phthalocyanines, porphyrin and Shiff's base type ligands as seen in Figure 3.5 (Arends et al. 2001).

Ligands bond with transition metal using the electron pairs. With this bonding ligand give electrons to the transition metal. Electropositive metal ion enters a second interaction with ligand to give accepted electrons from ligand to ligand. With this interaction metal gives electron and the bond between the metal and oxygen weakens. The weak bond between them causes the increasing susceptibility of reaction entrance of reactant. That is why transition metal complexes are used as catalysts. Transition

metal complexes catalyze the reaction and are considered to be good catalysts (Brunel et al. 1998).

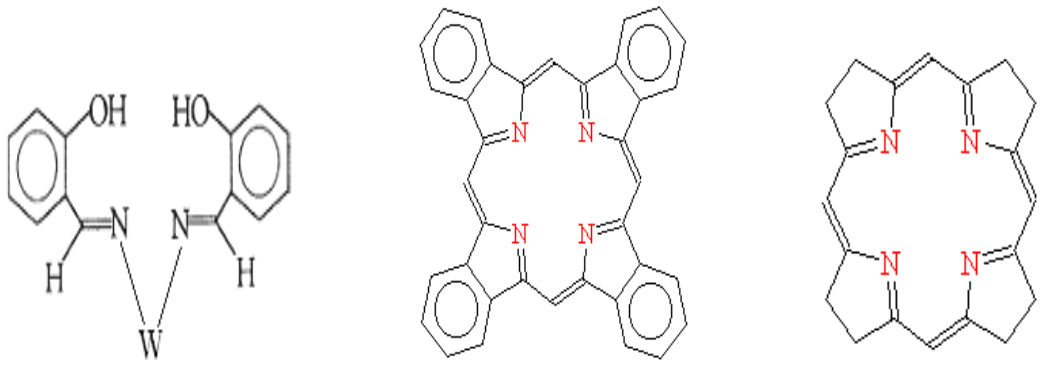

(a) (b) (c)

Figure 3.5. (a) Shiff's Base ligand (b) Phthalocyanine (c) Porphyrin (Source:Ramesh et al.2003, Ramesh et al. 1996)

In Figure 3.5 case (a), where

W = $-(CH_2)_2-$ (H_2salen)

$=-(CH(CH_3)-CH_2)-$ (H_2Salpn)

$=-(C_2H_4)\,NH\,(C_2H_4)-$ (H_2 saldien)

CHAPTER 4

DESIGN OF INTRAZEOLITE COMPLEXES

In the catalyst synthesis, the encapsulation of metal complexes into the zeolite cavities is known as a ship in a bottle procedure. These encapsulated catalysts are often referred to as zeozymes as they behave functionally similar to many enzyme catalysts in oxidation reactions (Maurya et al. 2002). Encapsulation of metal complexes is occurred in the super cages of the Y-zeolite. There are three possible approaches to incorporate metal complexes inside the pores or cavities of a zeolite. Encapsulated complexes are prepared by general flexible ligand method, ligand synthesis method inside the super cages of the Y-zeolite and zeolite synthesis method (Sheldon et al. 1998).

4.1. Flexible Ligand (FL) Method

A flexible ligand is able to diffuse freely through the zeolite pores as seen in Figure 4.1 and make complexes with a previously exchanged metal ion in the flexible ligand method (Velde et al. 2000). The resulting complex becomes too large and rigid to escape out of the cages. This approach is well adapted for encapsulation of metal-salen, salpn complexes, because the salen, salpn ligand offers the desired flexibility. Thus a large variety of metal salen, salpn complexes were prepared by FL method within the Y-faujasite (Chandra et al. 1998).

Zeolites Y is having pore opening of 7Å. Inside parts of zeolites have 12-13 Å supercage. The H_2 (salpn) ligand is having molecular dimensions less than 7 Å. It can easily diffuse inside the zeolite pore. The formed metal complex is too large to diffuse out (Brunel et al. 1998).

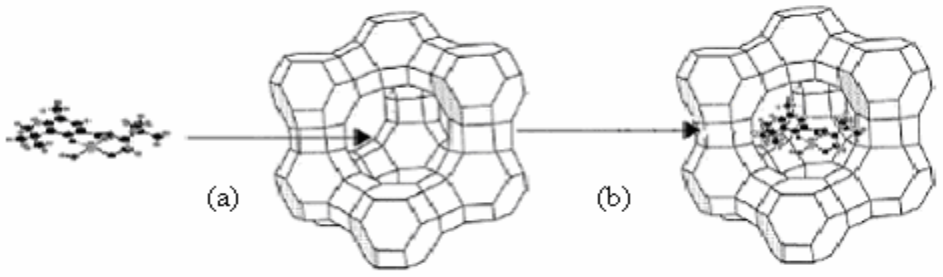

Figure 4.1. Flexible ligand method: (a) diffusion of flexible ligand (b) formation and encapsulation of complex in zeolite Y supercage
(Source: Velde et al. 2000)

The encapsulated metal complexes, which are prepared by flexible ligand method, are active catalysts for the decomposition of hydrogen peroxide, for the oxidation of phenol and selective oxidation reactions as seen in Table 4.1 by using H_2O_2 as oxidant.

Cr(III), Fe(III), Bi(III), Ni(II) and Zn(II) complexes of *N*,*N*-bis(salicylidene) propane-1,3-diamine (H_2 salpn as seen in Figure 4.2) encapsulated in Y-zeolite were prepared by flexible ligand method (Maurya et al. 2002). As H_2salpn has better flexible backbone, so its insertion into the cavity of the zeolite was better and hence, formation of metal complexes was enhanced. These encapsulated complexes are active catalysts for the decomposition of hydrogen peroxide and for the oxidation of phenol to catechol and hydroquinone with good selectivity.

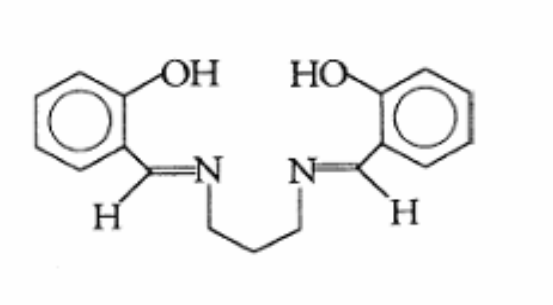

Figure 4.2. Structure of H_2salpn
(Source: Maurya et al. 2002)

Copper and manganese salens complexes encapsulated in the cavities of zeolites NaX and NaY to be used in selective oxidation reactions (Chandra et al. 1998). Salens carrying bulky substituents are retained to greater extent in the zeolite. The

stoichiometric and structural integrity of the salens is preserved on encapsulation in the zeolites.

4.2. Ligand Synthesis (LS) Method

In this method, ligand is synthesized inside the pores of zeolite. The synthesized complex becomes too large and rigid to escape out of the cages. This method is used in which the ligand itself is constructed inside the zeolite matrix. A metal exchanged zeolite is evacuated to a pressure of 10^{-5} torr. The molecules that constitute the ligand species (ligand precursors) are then adsorbed into the zeolite matrix in an inert atmosphere. The molecules form the ligands of interest and then make complexes with the metals, which present in the zeolite. The excess ligand precursors, the ligand present on the external surface and the complex present on the external surface are removed by soxhlet extraction (Nakagaki et al. 2000, Armengol et al. 1999).

Metal complexes which were prepared by ligand synthesis method were used for some oxidation reactions such as hydrocarbon and cyclohexane oxidation as shown in Table 4.1.

For hydrocarbon oxidation reactions, synthesis of, metalloporphyrins of Fe(III) and Cu(II) (zeolite-encapsulated metalloporphyrins) were prepared inside the large pores of the zeolite NaY (Nakagaki et al. 2000). For oxidation of cyclohexane, a series of Cu^{+2}-phthalocyanine and Co^{+2}-perfluorophthalocyanine has been prepared inside the pores of MCM-41 (MPcMCM-41) by ligand synthesis method. MCM-41 and zeolite Y was tested for oxidation of cyclohexane.

The void dimension of the porous host can play an important role in the catalytic activity and selectivity of MPc as oxidation catalysts because of differences between the planar and distorted conformation of the encaged MPc. The highest activity and selectivity of the CuPc complex is observed when incorporated inside Y zeolite according to MCM-41 for cyclohexane oxidation reaction (Armengol et al. 1999).

4.3. Zeolite Synthesis (ZS) Method

In the zeolite synthesis method, transition metal complexes, which are stable under the conditions of zeolite synthesis (high pH and elevated temperature etc.), are

included in the synthesis mixture. The resulting zeolite encapsulates the transition metal complex in its voids. The excess ligand and uncomplexed metal ions are major disadvantages of the first two methods. In order to avoid uncomplexed metal ions and excess ligands, the metal complexes are encapsulated during zeolite crystallization.

For oxidation of para-xylene, salen complexes of copper and manganese, encapsulated in the cavities of zeolite NaX have been investigated as catalysts for the aerobic oxidation of para-xylene. Significant conversion levels (up to 50-60%) were attained (Chandra et al. 1999).

Table 4.1**.** Data on heterogeneous catalysts used in oxidation reactions

Zeolite	**Method**	**Complex**	**Oxidation Reaction**	**References**
Na-Y	LS	Metalloporphyrins of Fe^{3+} Cu^{2+}	hydrocarbon	Nakagaki et al. 2000
Na-Y	LS	Cu^{2+} phtalocyanine	cyclohexane	Armengol et al. 1999
Na-Y	FL	Schiff base $Cu^{2+,}$ Mn^{2+}	phenol	Bennur et al. 2001
Na-Y	FL	Schiff base $Ru^{3+,}$ Co^{2+}	alfa-pinene	Joseph et al. 2002
Na-Y	FL	$Cu^{2+,}$ Mn^{3+} salens	styrene, phenol, p-xylene	Chandra et al. 1998
Na-Y	FL	Cu^{2+} salpn	phenol	Maurya et al. 2002
Na-Y	FL	Cr^{3+}, Fe^{3+}, Bi^{3+} saldien	phenol	Maurya et al. 2003
Na-X, Na-Y	FL, ZS	Copper (X_2-salen)	phenol	Chandra et al. 1998
Na-X	ZS	Fe^{3+} porphyrins	hydrocarbon	Rosa et al. 2000
Na-X	ZS	Mn^{3+} salen	Styrene	Varkey et al. 1998
Na-X	ZS	$Cu^{2+,}$ Mn^{+3} salens	p-xylene	Chandra et al. 1999
Na-X	ZS	$Cu^{2+,}$ Mn^{3+} salens	styrene, phenol, p-xylene	Chandra et al. 1998

The data on complexes prepared by flexible ligand method, ligand synthesis method, zeolite synthesis method for heterogeneous catalysts are given in Table 4.1. In the case of inorganic matrices, zeolites are an interesting choice because the pore diameters and geometry can introduce shape selectivity in the catalytic reaction.

In all reactions as seen in Table 4.1, acetonitrile is used as solvent. Solvents effect the reaction rate through competitive sorption and adsorption in the zeolite cavities. In addition, polarities, hydrophilicity, size of solvent molecule also play a role on reaction rate. Among the solvents CH_3CN, CCl_4, C_2H_5OH and pyridine used, CH_3CN has shown the best result in many oxidation reactions (Maurya et al. 2002b). These oxidation reactions proceed better in acetonitrile. The reason might be that reactant and hydrogen peroxide could reach active sites more easily than others. Oxidation reactions with hydrogen peroxide have strongly hydrophilic character. Most of substrates, such as monoterpenes have hydrophobic character. This causes a mismatch between them. To overcome this situation, bridging solvents such as acetnitrile, methanol are used (Sanderson et al. 2000).

CHAPTER 5

OXIDATION OF MONOTERPENES

5.1. Definition of Monoterpene

Essential oils are made up of many chemical constituents. No two oils are alike in their structure or their effects. Some of the main constituents found in essential oils are alcohols, esters, ketone, ether, phenol, terpenes..

Each of these can be broken down into numerous smaller units. For example terpene classification includes monoterpenes, sesquiterpenes, sesquiterpene lactones, Di-terpenes, etc. Terpene is a compound whose carbon skeleton can be divided into two or more units identical with the carbon skeleton of isoprene as seen in Figure 5.1 (Monteiro et al. 2004, Solomons 1988). The basic building block of many essential oils is a five-carbon molecule called an isoprene. Most essential oils are built from isoprene. When two isoprene units link together, they create a monoterpene; when three join, they create a sesquiterpene; and so forth. Triterpenoids are some of the largest molecules found in essential oils. They consist of 30 carbon atoms or six isoprene units linked together.

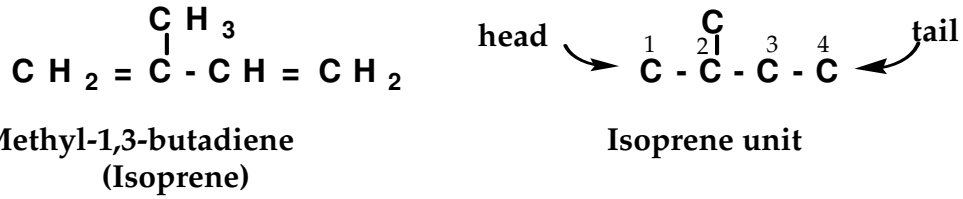

Figure 5.1. Isoprene structure

(Source: Monteiro et al. 2004, Solomons 1988)

Oxygenated monoterpenes are major components in the essential oils. Carvacrol, thymol and *p*-cymene are *p*-menthane type of aromatic monoterpenes, which can be found in the essential oils of aromatic plants (Martin et al. 1999).

Monoterpenes are widely used in pharmaceutical, cosmetic and food industries as active components. Some reactions of considerable commercial importance are epoxidation of alfa pinene to alfa pinene oxide, which is an intermediate used in the synthesis of several sandalwood fragrances; epoxidation of limonene to limonene oxide, used to treat rhinitis; oxidation of carvacrol or thymol to thymoquinone, which has antitumor and hepatoprotective effects (Skrobot et al. 2003).

5.2. Chemical Composition of Essential Oils

Different molecules in the same essential oil can exert different effects. This is because the chemical structure of an essential oil determines its function. For example, the phenols generally create antibacterial activity. Carvacrols have anti-inflammatory activity and Limonines are antiviral (Monteiro et al. 2004).

The chemical composition of essential oils depends on climatic, seasonal, and geographic conditions, harvest period, and distillation technique (Baydar et al. 2003). In literature, the chemical composition of the some essential oils was studied by gas chromotography (GC).

The aerial parts of wild oregano (*Origanum minutiflorum*) (endemic in Turkey), oregano (*Origanum onites*), black thyme (*Thymbra spicata*) and wild savory (*Satureja cuneifolia*) were collected wild during the flowering stage from the south western part of Turkey. The major constituent of the oils determined by GC was carvacrol (85.9% in *O. onites,* 84.5% in *O. minutiflorum*, 75.5% in *T. spicata* and 53.3% in *S. cuneifolia*) (Baydar et al. 2003). The essential oil components identified are given in Table 5.1. Eight major constituents were determined representing 97.4% in wild oregano, 97.1% in oregano, 99.0% in black thyme and 93.1% in wild savory (Baydar et al. 2003).

The chemical composition *Thymus revolutus*, an endemic plant of Turkey, were analyzed by GC. Twenty-two components were identified, and carvacrol was found as a predominant compound in the oil. Twenty-two components were identified in the oil, representing 98.15% of the total oil. The major components were carvacrol (43.13%), alfa-terpinene (20.85%), *p*-cymene (13.94%), caryophyllene (5.40%) and thymol (4.52%) (Karaman et al. 2001).Several earlier studies on another Turkish *Thymus* showed that the main components of the oils were carvacrol and thymol in *Thymus* (Tumen et al. 1994).

In the GC–MS analysis of the oil of *Thymus migricus* from Ağrı, Turkey 50 compounds, representing 97% of the total oil was characterized. Carvacrol (35%) being the major component in essential oil. In the other oils obtained from *Thymus migricus* samples collected from Van, Turkey province 40–75 compounds, representing 98–99% of the oils, were characterized. Thymol (35–44%) was found as the major component (Canbeşer et al. 2001).

Table 5.1. Chemical composition of the essential oils (% total peak area)
(Source: Baydar et al. 2003)

	Essential oil components (%)			
	Wild oregano	Oregano	Black thyme	Wild savory
Myrcene	1.5	1.3	1.3	2.1
a-terpinene	0.8	0.9	1.1	2.1
c-terpinene	3.3	3.9	11.5	27.4
p-cymene	4.2	2.9	9.2	7.3
Bornylacetate	0.8	0.4	0.1	0.1
Borneol	0.5	0.5	0.1	0.7
Thymol	1.7	0.2	0.1	0.1
Cavracrol	84.5	85.9	75.5	53.3

The major components of essential oils from oregano and thymus species in Turkey are thymol and/or carvacrol. Thymol and carvacrol can be transformed into more valuable product thymoquinone by oxidation reactions.

5.3. Oxidation of Monoterpenes

Chemical transformation of abundant and cheap products into novel and more valuable compounds can be achieved by liquid-phase oxidation reactions using hydrogen peroxide as clean oxidant and zeolite encapsulated metal complexes as heterogeneous catalyst (Skrobot et al. 2003). Hydrogen peroxide is a clean oxidant because it is easy to handle and its reaction produces only water as by-product (Arends

et al, 2001). Catalytic oxidation of aromatic monoterpenes with hydrogen peroxide is a reaction of industrial importance (Martin et al. 1999).

Activation of the catalyst occurs upon addition of hydrogen peroxide or molecular oxygen (clean oxidants) to generate a high valent metal-oxo species. These catalytic metallo-oxidants or green oxidants are able to effectively and selectively oxidize a multitude of organic substrates, phenols into their corresponding oxygenates at low temperatures (<100°C) and pressures (< 2 atm) with mild condition. In gas phase reaction using moleculer oxygen and in liquid phase reaction using hydrogen peroxide as an unstable oxidizing agent with mild conditions are very useful (Sanderson et al. 2000).

Recently, many publications have dealt with the antitumor and hepatoprotective activity of thymoquinone (Badary et al. 1999). Since the natural resources of thymoquinone is limited only to certain plant resources such as *Nigella sativa, Callitris articulata* and *Munardo fistulasoi,* there is a growing interest for its production by the transformation of the other chemicals. Thymoquinone has a commercial value considerably higher than its precursors (thymol and carvacrol) found in thyme essential oil. It can be obtained by catalytic oxidation of thymol and carvacrol. Table 5.2 summarizes the studies of oxidation monoterpenes and essential oils using homogeneous and heterogeneous catalysts in literature.

Oregano (*Origanum vulgare*) is an aromatic plant very rich in essential oil which in turn is an important natural resource of thymol and carvacrol. Fifteen compounds were identified and quantified by GC–MS to represent 98.8% of the oil. The essential oil was particularly rich in thymol and carvacrol (47.5 and 25.1%) and p-cymene (21.4%). The alfa terpinene (2.0%) was identified in a relatively large quantity, while all the other constituents amounted to less than 1%, respectively. This oregano essential oil were easily oxidized by hydrogen peroxide to oil containing thymoquinone (19.1-53.3%) as the main component in the presence of Fe(III) meso-tetraphenylporphyrin or Fe(III) phthalocyanines complexes as seen in Table 5.2 (Milos et al. 2001). The carvacrol oxidation with hydrogen peroxide was also studied using Mn(III) porphyrin complexes and keggin-type tungstoborates (Martin et al. 1999, Santos et al. 2003). Oxidation of carvacrol yielded a mixture of benzoquinones containing a small amount of thymoquinone for keggin-type tunstoborates where as for Mn(III) porphyrin oxidation of carvacrol selectively yielded thymoquinone.

There are few studies on monoterpene oxidation with heterogeneous catalyst in literature. By using zeolite encapsulated metal complexes thymoquinone can be obtained by catalytic oxidation of carvacrol and thymol. Oxidation of carvacrol and thymol in the presence of Y-zeolite-entrapped Mn(III) tetra (4-N-benzylpyridyl) porphyrin was performed (Skrobot et al. 2003). The oxidation of carvacrol (<25% conversion) and thymol (<18% conversion) gave thymoquinone with 100% selectivity.

Table 5.2. Data on heterogeneous and homogeneous catalysts used in monoterpene and essential oil oxidation reaction

Catalyst type	Complex	Oxidation reaction	References
Heterogeneous	Y zeolite-entrapment Mn^{3+} tetra (4N benzylpyridyl) porphyrin	Monoterpene (carvacrol, thymol)	Skrobot et al. 2003
Heterogeneous	Keggin type tunstoborates	Monoterpene (carvacrol, thymol, p-cymene, alfa-terpinene)	Santos et al. 2003
Homogeneous	Mn^{3+} porphyrins	Monoterpene (carvacrol, thymol, p-cymene, alfa-terpinene)	Martin et al. 1999
Homogeneous	Fe^{3+} meso-tetraphenylporphyrin, phthalocyianine	oregano essential oil	Milos et al. 2001

5.4. Catalytic Monoterpene Oxidation with Hydrogen Peroxide

Activation of hydrogen peroxide can be divided into two parts: Catalytic activation by transition metal complexes and direct activation (unproductive reaction), Fenton chemistry (Bregeault et al. 2003). For these activations, two general types of mechanisms have been postulated for the decomposition of hydrogen peroxide. The first is fenton reaction mechanism which is free radical mechanism (homolytic pathway) second is the peroxide complex mechanism (heterolytic pathway), (Salem et al. 2000).

Oxidations with H_2O_2 can involve homolytic pathways via free radical intermediates and/or heterolytic oxygen transfer processes as seen in Figure 5.2 (Sheldon et al. 1998). In Figure 5.2, carvacrol is used as reactant which is the major monoterpene component of many essential oil.

Heterolytic oxygen transfer process can be divided into two types based on the active intermediate: a peroxometal or an oxometal complex. Peroxometal pathways usually involve early transition elements with d^0 configuration, e.g. Mo(VI), W(VI), V(V), Ti(IV). Late or first row transition elements, e.g. Cr(VI), V(V), Mn(V), Ru(VI), Ru(VIII), Os(VIII), generally employ oxometal pathways. Some elements, e.g. vanadium, can employ oxometal or peroxometal pathways depending on the reactant (Arends et al. 2001).

In the presence of transition metal complexes oxidation reactions with hydrogen peroxide are direct activation (unproductive oxidation) and productive oxidation reactions as seen in Figure 5.3 and water is only by product. Catalysts (transition metal complexes) are transferred oxygen from hydrogen peroxide to the reactant or substrate by a homolytic cleavage of the metal oxygen bond (Salem et al. 2000).

Homolytic Pathways:

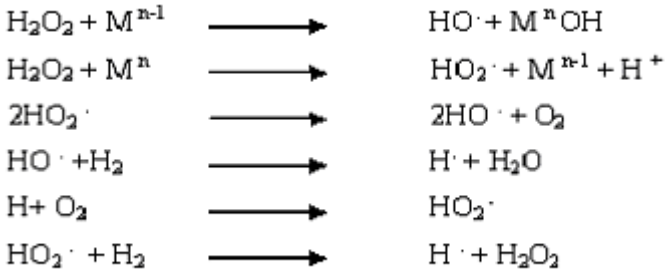

Heterolytic Pathways:

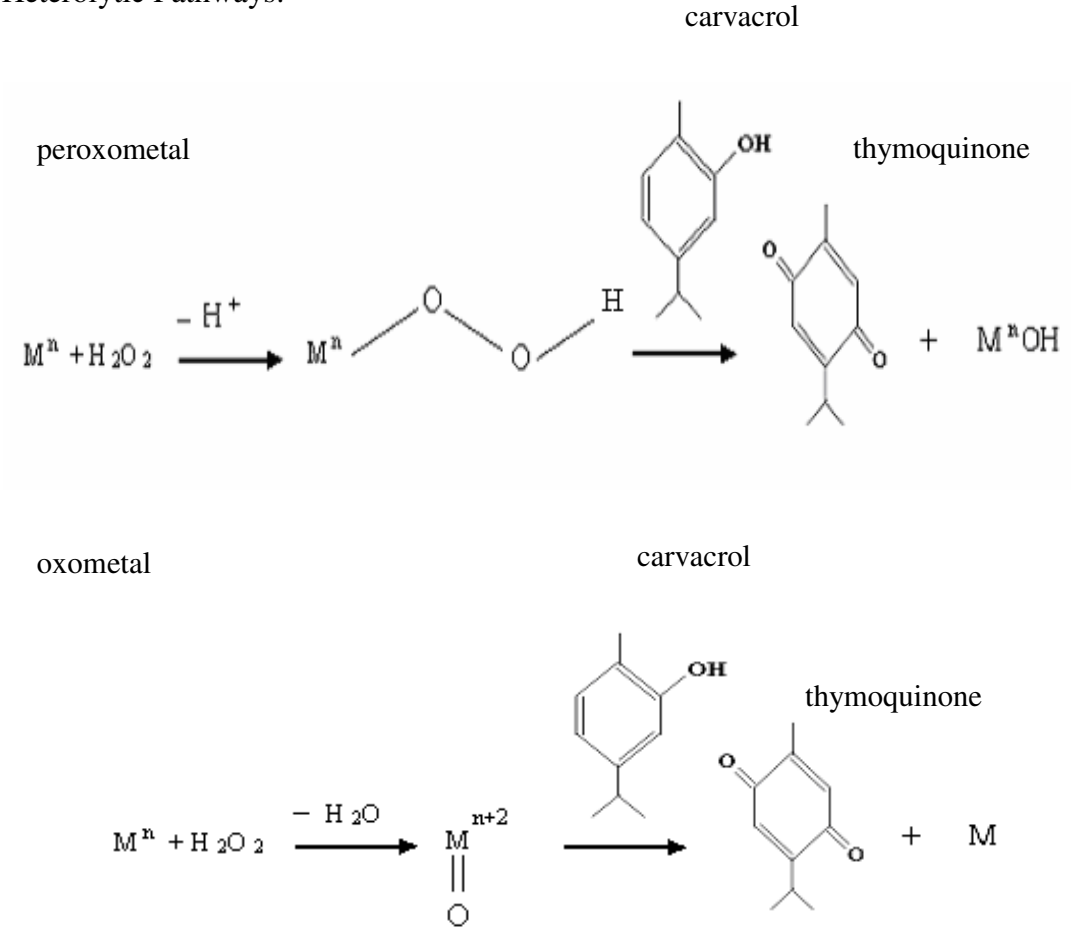

Figure 5.2. Proposed possible oxidation mechanism with hydrogen peroxide

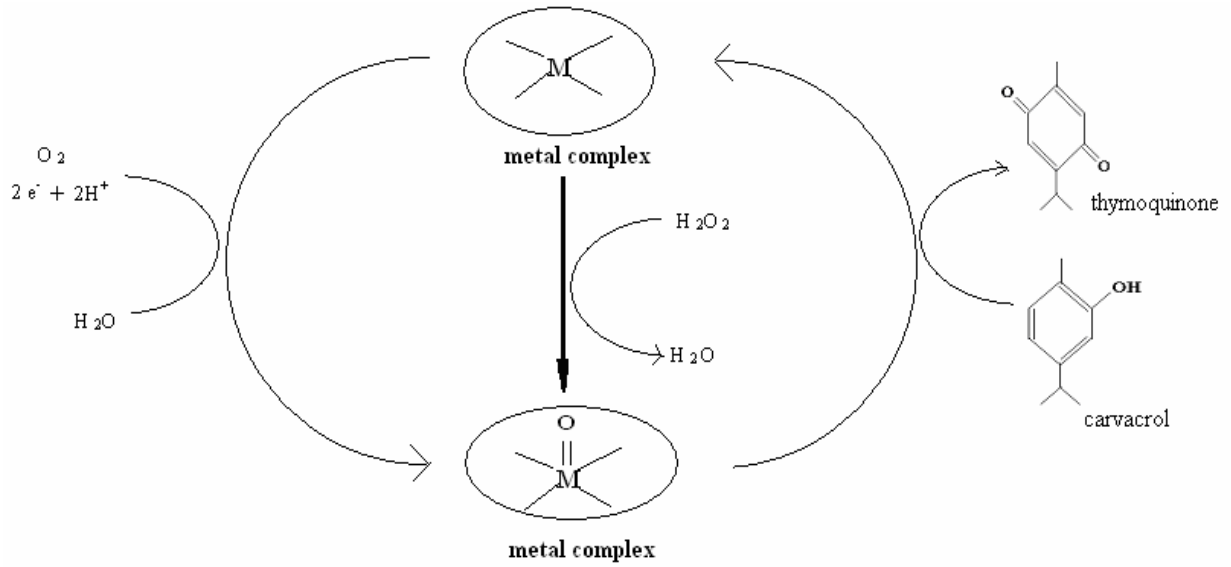

Figure 5.3. Oxidation of carvacrol with hydrogen peroxide by using metal complex

CHAPTER 6

EXPERIMENTAL

6.1. Materials

Metal nitrates (nitrates of Cr(III), Fe(III), Bi(III), Ni(II), Zn(II)), carvacrol (5-isopropyl-2-methylphenol), thymol (2-isopropyl-5-methylphenol), thymoquinone (2-isopropyl-5-methyl-p-benzoquinone), salicylaldehyde, 1,3-diamino-propane and hydrogen peroxide (30%) were purchased from Sigma-Aldrich. Other reagents and solvents used were HPLC grade and obtained from Sigma-Aldrich. Essential oil was purchased from Arifoğulları company. Zeolite-NaY (CBV100, SiO_2/Al_2O_3 5.1) that contained 13.0 wt% Na_2O was purchased from Zeolyst International Company in the form of powder with the sizes less than one micron. The surface area of the zeolite powder was 900 m^2g^{-1}. The unit cell formula of this sample was $Na_{54}(AlO_2)_{54}(SiO_2)_{138}$ when dehydrated. Zeolite-NaY was activated at 500 °C in an oven for at 5h and cooled to room temperature in a desiccator before use.

6.2. Methods

6.2.1. Catalyst Preparations

H_2salpn, metal exchanged zeolite Y, and encapsulated complexes were prepared by following a procedure similar to one described in the literature (Maurya et al. 2002).

6.2.1.1. Preparation of Ligand (H_2Salpn)

Salicylaldehyde (12.2 g, 0.1 mol) was dissolved in 65 ml methanol and mixed with a solution of 1,3-diamino-propane (3.65 g, 0.05 mol) in 25 ml methanol. Solution was refluxed in a water bath for 1 hour. After reducing the volume of solution to 50 ml, flask was kept at ambient temperature for 2 hours. Yellow shining plates were filtrated,

washed with 10 ml cold methanol and dried. Finally, the ligand was recrystallized from methanol to give pure product. The melting point of ligand was found by differential scanning calorimetric analysis (DSC). DSC analysis was conducted using Shimadzu DSC50 types of instrument. Run was carried out up to 600 ^{o}C at 10 ºC/min heating rate and nitrogen flow rate with 3 mg of sample.

6.2.1.2. Preparation of Metal Exchanged Zeolite Y

NaY-zeolite (5 g) was suspended in 300 ml deionized water containing 0.01 M of metal (Cr(III), Fe(III), Bi(III), Ni(II), Zn(II)) nitrates. The mixture was heated to 60 ºC while stirring for 24 hours. The solid was filtrated, washed with hot distilled water till the filtrate was free from any metal ion content and then dried for 24 hours at 90 ºC in air.

6.2.1.3. Preparation of Encapsulated Complexes

The encapsulated metal complex was prepared by general flexible ligand method. A total of 5g metal exchanged Y zeolite and 10 g of ligand were mixed in round bottom flask. The mixture was heated at 100 ºC overnight (19 hours) in an oil bath with stirring. The ligand was melted at that temperature and acted as a solvent as well as a reactant. The resulting material was taken out and soxhlet extracted with methanol till the complex was free from unreacted excess ligand (at least 62 hours). The uncomplexed metal ions present in the zeolite were removed by exchanging them with 0.01 M aqueous NaCl solution for 5 hours. The resulting solid then was washed with hot distilled water till no precipitation of AgCl on reacting filtrate with $AgNO_3$ was observed. The colored solid was dried at 90 ºC for 24 hours.

6.2.2. Catalyst Characterization

X-ray diffraction (XRD) patterns of the samples were recorded on a Philips X'pert Pro X-ray diffractometer with Cu Kα radiation. Infrared spectra in the region 400-4000 cm^{-1} were recorded in KBr pellets using a Shimadzu 8101 FT-IR spectrophotometer. The metal contents in the products were determined by an

inductively coupled plasma spectrometer (ICP, Varian 8410). Scanning electron micrographs were recorded on a Philips XL 30S FEG. Nitrogen physisorption studies were performed at 25 °C using Micromeritics ASAP 2010 model static volumetric adsorption instrument using nitrogen at 77 K. The samples were dried in oven at 200 ºC for 3 hours prior to degassing and degas conditions were adjusted as 350 ºC and 24 hours under 5µmHg vacuum. The specific surface area was calculated by the Langmuir method. Micropore volumes, of the same samples were calculated by Horvath-Kawazoe method.

Thermal gravimetric (TGA) analyses were conducted using Shimadzu TGA-51/51H types of instrument. Approximately 10 mg sample was heated at 10 ºC /min under 40 ml/min nitrogen purge stream up to 800 ºC in the TGA studies. TGA measures weight loss of the sample as it was heated to elevated temperatures.

6.2.3. Catalytic Activity

6.2.3.1. Decomposition of Hydrogen Peroxide

An amount of 0.025 g of encapsulated catalyst was added to an aqueous solution of 30% H_2O_2 (5.5 g, 0.049mol) at room temperature (25 ºC) and the reaction mixture was stirred for the predetermined time (1 hour or 2 hours). At the end of the reaction, the catalyst was filtered and the filtrate was diluted to 250 ml with deionized water. Ten milliliters of this solution was withdrawn and after addition of 20 ml of 2.5 M H_2SO_4 and 20 ml of deionized water, it was titrated against standard 0.02 M $KMnO_4$ solution. Calculation procedure of percentage hydrogen peroxide decomposition data was given an Appendix A.

6.2.3.2. Oxidation of Carvacrol and Thymol

Carvacrol and thymol oxidations were carried out at 60 ºC in a three-necked flask (250 ml) equipped with a magnetic stirrer, a reflux condenser and a temperature controller. The certain amount of carvacrol (4.4 g, 0.029 mol), and 16 ml acetonitrile were added successively into the flask. Then, appropriate amount of 30 wt. % aqueous H_2O_2 (0.029 mol) was added for the required carvacrol-to-hydrogen peroxide molar

ratio. After heating the mixture containing carvacrol, acetonitrile and hydrogen peroxide to 60 ºC certain amount of catalyst was added to the reaction mixture and reaction was started. The reaction was monitored by taking aliquots at different times. Samples from the reaction mixtures were analyzed by high performance liquid chromatography (HPLC). The samples were centrifuged to remove the catalyst before analysis. Since quinones expected from the reaction mixture undergo facile formation of radicals when exposed to light. Immediately after sample collection, vials containing reaction mixture were covered by aluminum foil, to protect them from light.

HPLC analyses were carried out with a method similar to the one described in the literature (Ghosheh et al. 1999). An Agilent 1100 HPLC system equipped with a reversed phase C18 column (250 mm x 4.6 mm I.D., 5 μm particle sizes, Lichrospher®) was used for HPLC analysis. Aliquots of 20 μl were injected and separation was carried out with an isocratic mobile phase consisting of methanol-water (60:40, v/v) with a flow-rate of 1 ml min^{-1} and at 30 ºC column temperature. The detection wavelengths were 254 nm for detecting carvacrol, thymol, thymoquinone, and 294 nm for thymohydroquinone, which has a low absorptivity at 254 nm. These wavelengths were chosen since they gave the maximum absorbance. Prior to injection of a sample, the column was equilibrated with the mobile phase at a flow-rate of 1 ml min^{-1} for at least 20 min or until a steady baseline was obtained. Percentage of carvacrol conversion and thmoquinone yield in the reaction mixtures were estimated from the calibration curves (Appendix B).

6.2.3.3. Heterogeneity Tests

To test if metal complex was leaching out from the catalyst, the reaction mixture was filtered hot. The filtration was performed at the reaction temperature in order to prevent a possible readsorption of leached metals. The filtrate was monitored by HPLC analysis to check the progress of the reaction in homogeneous phase. The heterogeneity of the prepared catalysts was also evaluated by digesting the filtrate after each reaction completion. The filtrate was digested in a teflon beaker by the addition of HNO_3 after all the organic solvent was completely evaporated. Metal contents of digested residue for all catalysts were determined using inductively coupled plasma (ICP) technique.

These tests were performed in detail especially for Cr(salpn)-NaY and Fe(salpn)-NaY catalysts.

CHAPTER 7

RESULTS AND DISCUSSIONS

7.1. Catalyst Characterization

Prepared catalysts were characterized by Inductively Coupled Plasma (ICP), Scanning Electron Microscopy (SEM), X-ray Diffraction (XRD), Fourier Transform Infrared (FTIR) Spectroscopy, pore volume, surface area measurement techniques and thermal gravimetric analyses (TGA).

7.1.1. Elemental Analysis by Inductively Coupled Plasma Analysis

Encapsulation of Cr(III), Fe(III), Bi(III), Ni(II) and Zn(II) complexes of H_2 salpn in NaY-zeolite was performed using flexible ligand method. In the literature, this method was described and used by several researchers (Maurya et al. 2002; Chandra et al. 1998, Balkus et al. 1995). The ligand molecule (H_2 salpn), which was flexible enough to diffuse through the zeolite channels, reacted with the previously ion exchanged metal ions in the zeolite supercage to obtain the encapsulated metal complexes. The final catalysts were purified from unreacted ligand and surface complexes by extensive soxhlet-extraction with methanol. The remaining uncomplexed free metal ions re-exchanged from the zeolite lattice by NaCl treatment. During the purification process catalyst samples preserved their initial color, indicating that metal complexes were formed in the zeolite cavities and the formed complexes were too large to diffuse out of the channels of zeolite.

The color and metal content of various catalysts, which was estimated by ICP technique, were presented in Table 7.1. The metal ion contents determined after encapsulation were due to the presence of metal complexes in zeolite framework. Low percentage of metal content was in good agreement with the results reported earlier in the literature (Maurya et al. 2002).

Table 7.1. Metal content of encapsulated catalysts.

Catalyst	Metal content (wt. %)	Color
Cr(salpn)-NaY	1.74	Pale blue-green
Fe(salpn)-NaY	1.36	Pale brown
Bi(salpn)-NaY	1.04	White
Ni(salpn)-NaY	0.15	Off white
Zn(salpn)-NaY	0.51	Off white

The prepared catalysts were further characterized by using SEM, XRD and FTIR techniques to confirm the encapsulation of metal complexes inside the zeolite supercage.

7.1.2. Scanning Electron Microscopy (SEM) Analysis

SEM micrograph can be used to observe changes in the morphology of zeolite after encapsulation of the metal complexes. It was also possible to observe the excess complexes, if any, located on the external surface of zeolite.

The SEM images of M(salpn)-NaY were similar to those observed for NaY, indicating that they possessed the same morphology, i.e., the framework around the guest molecule M(salpn) was faujasite-Y (Figure 7.1). The Si/Al ratio of the catalyst samples was 2.5±0.1, ascertained by EDS. It was observed that the Si/Al ratio (2.5±0.1) of the catalyst samples did not change comparing with the Si/Al ratio (2.5±0.1) of NaY zeolite. This result confirmed that there was no dealumination of the zeolite during catalyst preparation. SEM micrographs of NaY and Cr(salpn)-NaY Ni(salpn)-NaY, Fe(salpn)-NaY, Zn(salpn)NaY and Bi(salpn)-NaY were shown in Figure 7.1. In the SEM of catalyst samples, no surface complexes were seen and the particle boundaries on the external surface of zeolite were clearly distinguishable. These micrographs revealed the efficiency of purification with soxhlet-extraction for complete removal of extraneous complexes, leading to well-defined encapsulation in the cavity only (Skrobot et al. 2003, Varkey et al. 1998, Xavier et al. 2004, Maurya et al. 2003).

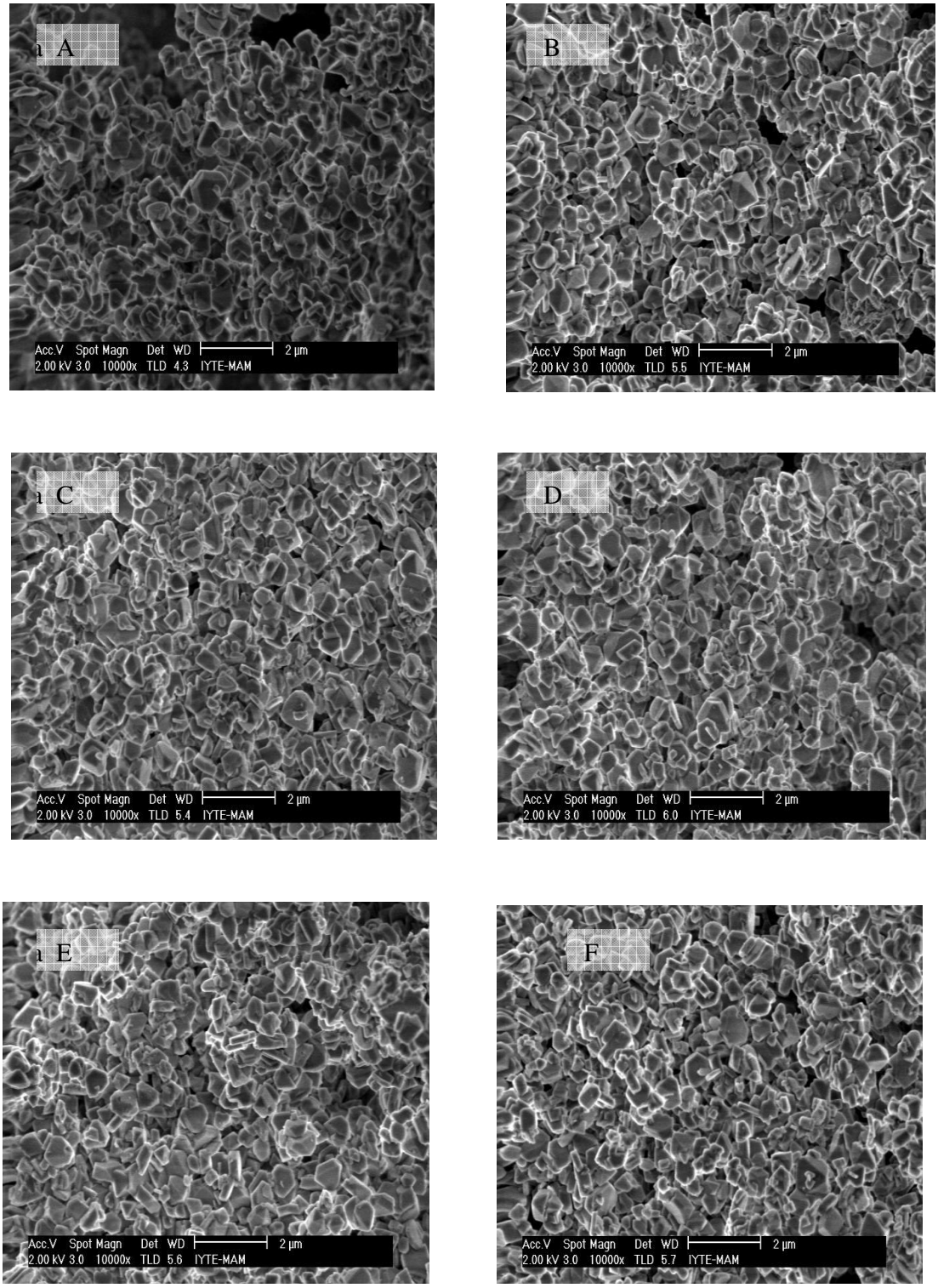

Figure 7.1. Scanning electron micrographs of NaY (A) and Cr(salpn)-NaY (B) Bi(salpn)-NaY (C) and Fe(salpn)-NaY (D), Ni(salpn)-NaY (E) and Zn(salpn)-NaY (F)

7.1.3. X-ray Diffraction (XRD) Analysis

The XRD patterns of NaY-zeolite, M-NaY (M=Ni(II), Zn(II), Cr(III), Fe(III), Bi(III)) and their complexes of H_2salpn (L) encapsulated in NaY-zeolite were recorded at 2θ values between 5 and 60º. These observations indicated that zeolite framework has not undergone any significant structural change during the encapsulation of M-H_2salpn and the crystallinity of NaY-zeolite was preserved, though, only slight change in the intensity of the bands was observed. Slight change in the intensities of the peaks suggested that the supercages of the zeolite were able to store these complexes without any strain (Maurya et al. 2002). The main framework of the zeolite was not damaged. Moreover, no specific crystalline patterns were seen for the encapsulated complexes; this might be because of their fine distribution in the lattice (Xavier et al. 2004). All samples exhibited patterns, which could be indexed to NaY and not to the complex. This indicated that the crystallinity and morphology of zeolite was preserved during encapsulation process.

XRD can be used to investigate the distribution inside the zeolite matrix. An empirically derived relationship exists between the relative peak intensities of the 331, 311, and 220 reflections and the location of small cations in NaY-zeolite (Balkus et al. 1995). Cations were randomly distributed within the lattice if $I_{331}>I_{220}>I_{311}$. From a comparison of XRD patterns it was seen that little changes occurred in the relative intensities of the peaks at 331, 311 and 220 reflections upon encapsulation of metal (Ni, Fe, Zn, Bi, Cr) complexes of H_2salpn (L) in zeolite-Y. Fan et al. (2003) and Joseph et al. (2002) also observed and used these relative intensities changes for the explanation of encapsulation.

XRD patterns of NaY, ligand (H_2 salpn) and all encapsulated complexes were shown in Figure 7.2. Figure 7.2 shows that samples have the faujasite topological structure with high crystallinity. Upon complexing metal ions with salpn ligand and further soxhlet-extracting, the faujasite structure basically remained unchanged. This indicated that complexing and extraction processes did not have strong influence on the structure of the zeolite. Nevertheless, slight modification occurred, as confirmed by the alteration of the relative intensity of the peaks at 220 and 311 reflections (2θ of about 10 and 12°, respectively). For Cr-NaY, I_{220} was slightly higher than I_{311}, whereas after being coordinated to salpn, I_{220} became lower than I_{311}. In BiNaY and Bi(salpn)-NaY

catalyst these peaks were not observed. This was typical for the formation of large transition metal complex ion in the supercage of zeolite Y (Fan et al. 2003).This can also be verified by FTIR spectroscopy.

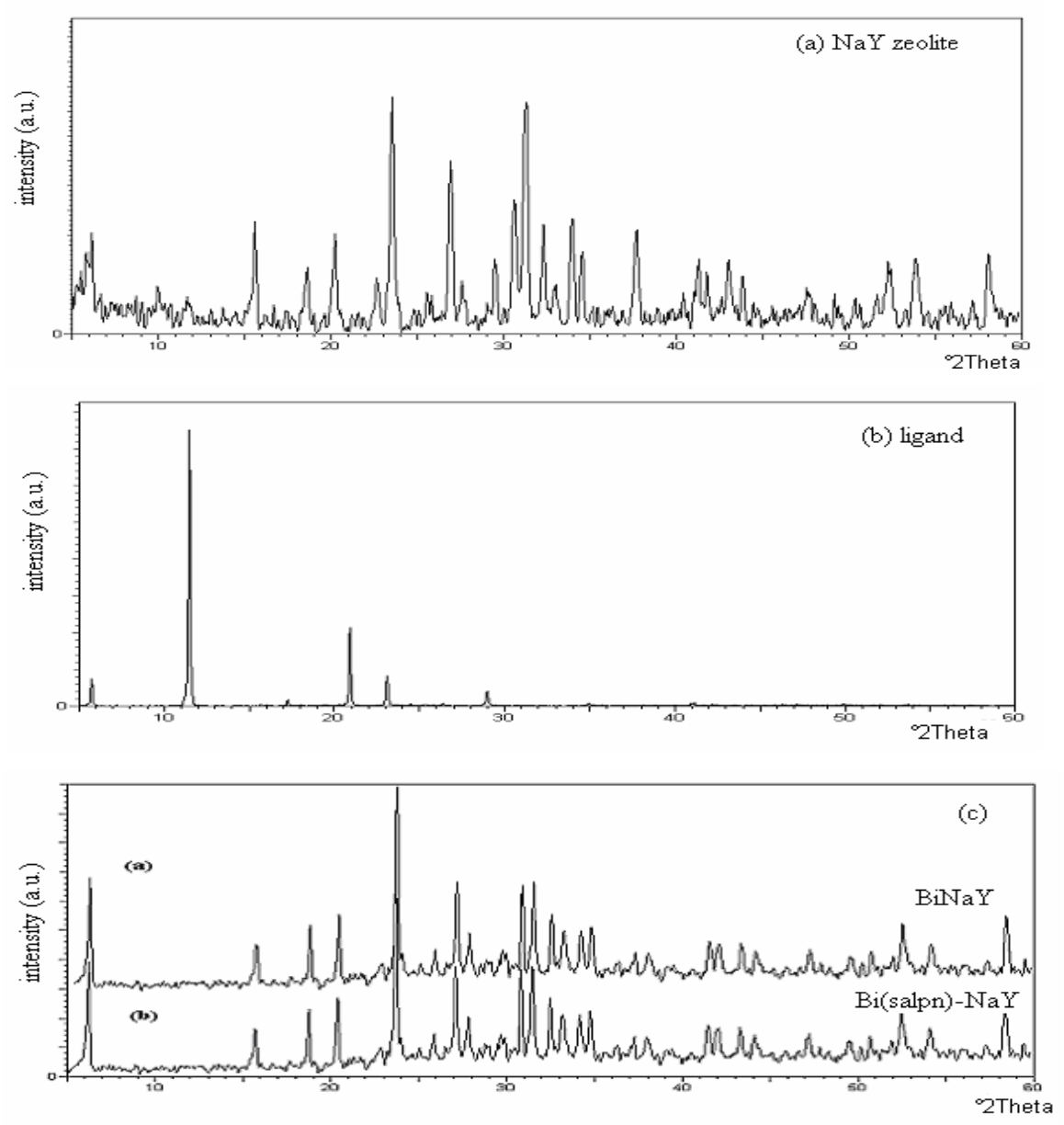

Figure 7.2. XRD patterns of NaY zeolite (a), ligand (H_2 salpn) (b), BiNaY, Bi (salpn)-NaY (c), Ni NaY, Ni (salpn)-NaY (d), Zn NaY, Zn (salpn)-NaY (e), Cr NaY, Cr (salpn)-NaY (f), Fe NaY, Fe (salpn)-NaY (g)

(cont.on next page)

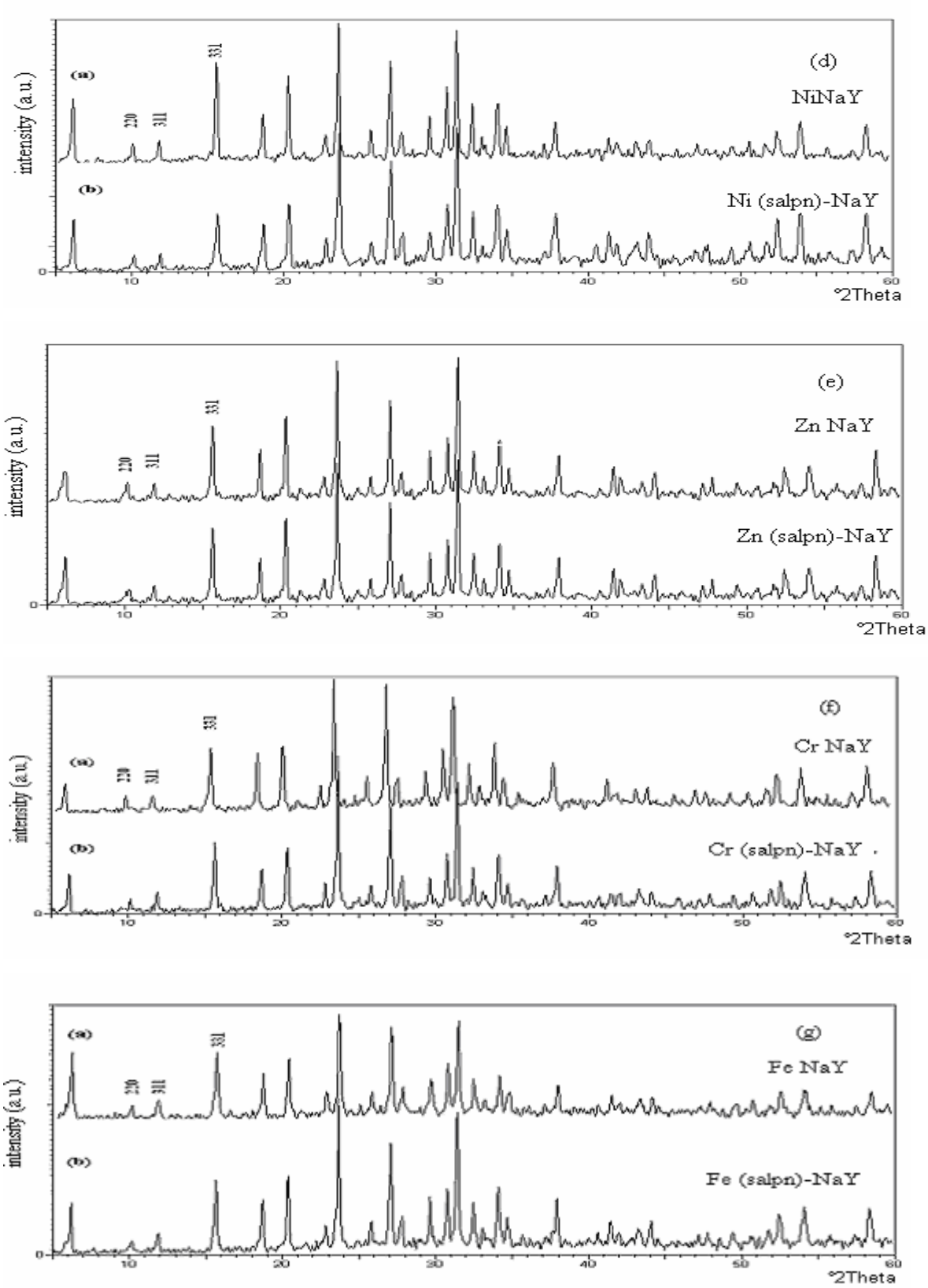

Figure 7.2 (cont.)

7.1.4. FTIR Spectroscopy Analysis

IR spectra of NaY zeolite and metal-exchanged zeolites showed strong zeolite lattice bands in the range 450-1200 1/cm as shown in Figure 7.3. The strong and broad band at the region 1000 1/cm could be attributed to the asymmetric stretching vibrations of $(Si/Al)O_4$ units. The broad bands at the region 1650 and 3500 1/cm were due to lattice water molecules and surface hydroxylic groups. No shift of zeolite lattice bands was observed in the spectra of encapsulated complexes given in Figure 7.4, which further implies that the zeolite framework has remained unchanged upon the encapsulation of complexes.

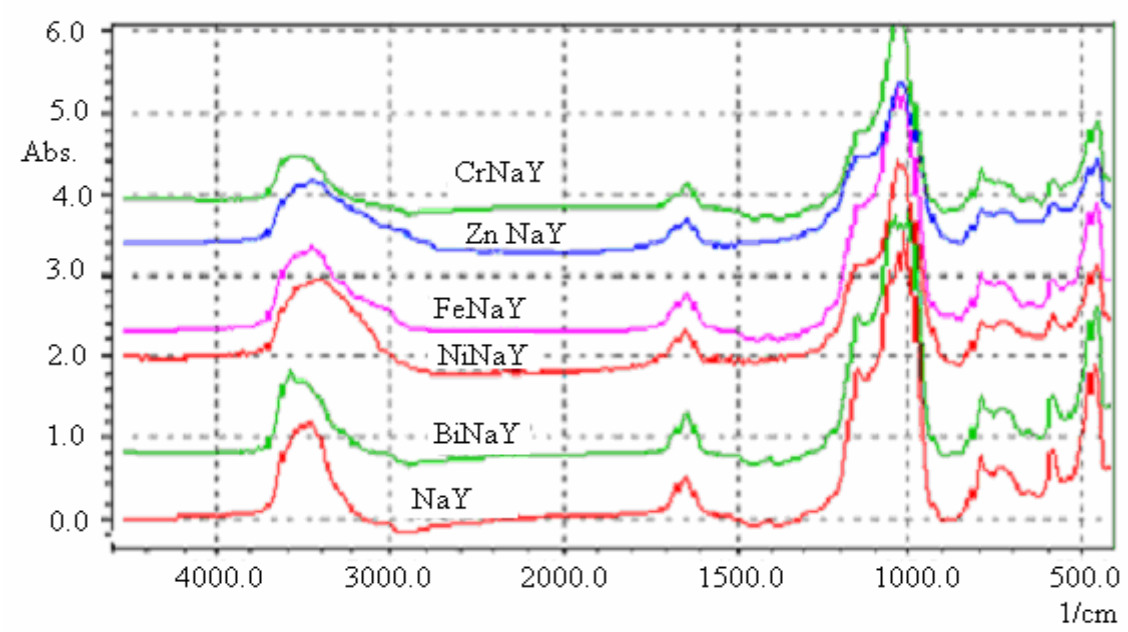

Figure 7.3. IR spectra of zeolite NaY, CrNaY, ZnNaY, FeNaY, NiNaY, BiNaY

A partial list of the IR spectra results of ligand (Figure 7.5), encapsulated complexes and free complexes (Figure 7.4) were given in Table 7.2. The IR spectra of ligand exhibited a broad band between 2400-2700 1/cm region due to hydrogen bonding between phenolic hydrogen and azomethine nitrogen atoms. The multiple bands around 2900 1/cm in IR spectrum of ligand were due to the presence of $-CH_2-$ group. Absence of the band was due to hydrogen bonding and coordination of oxygen to the metal after proton removal. In IR spectra of encapsulated complexes the zeolite bands were dominant. Only weak bands were observed for zeolite-encapsulated complexes due to lower complex concentration. The coordination in the pores could be identified from the

bands observed in the region 1200–1600 1/cm where zeolite had no bands. However, the bands due to complexes were weakly intense due to their low concentrations in the lattice as explained by Xavier et al. (2004).

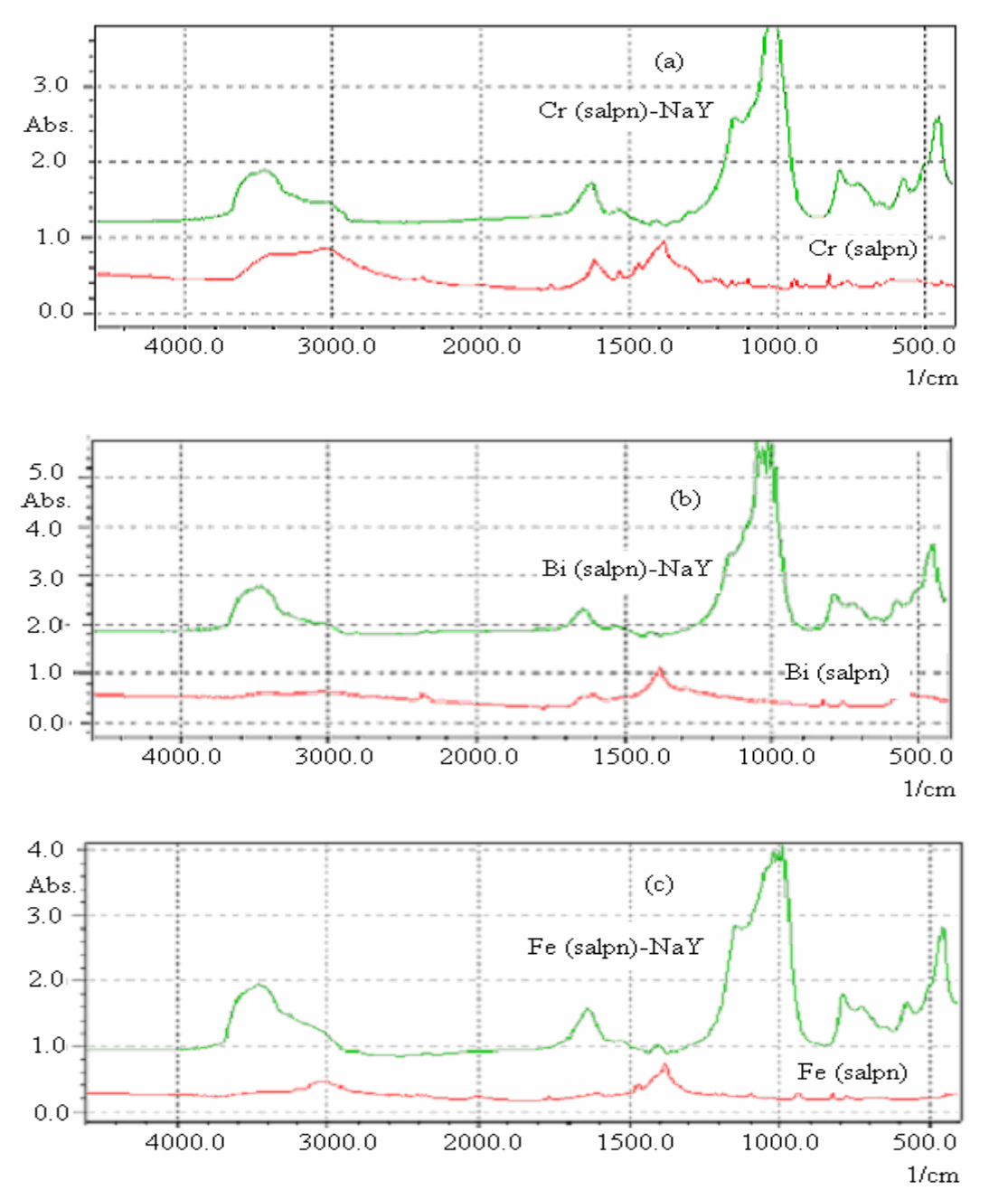

Figure 7.4. IR spectra of Cr(salpn)-NaY, Cr (salpn) (a), Bi(salpn)-NaY, Bi(salpn) (b), Fe (salpn)-NaY, Fe(salpn) (c), Ni(salpn)-NaY, Ni(salpn) (d), Zn (salpn)-NaY, Zn (salpn) (f)

(cont. on next page)

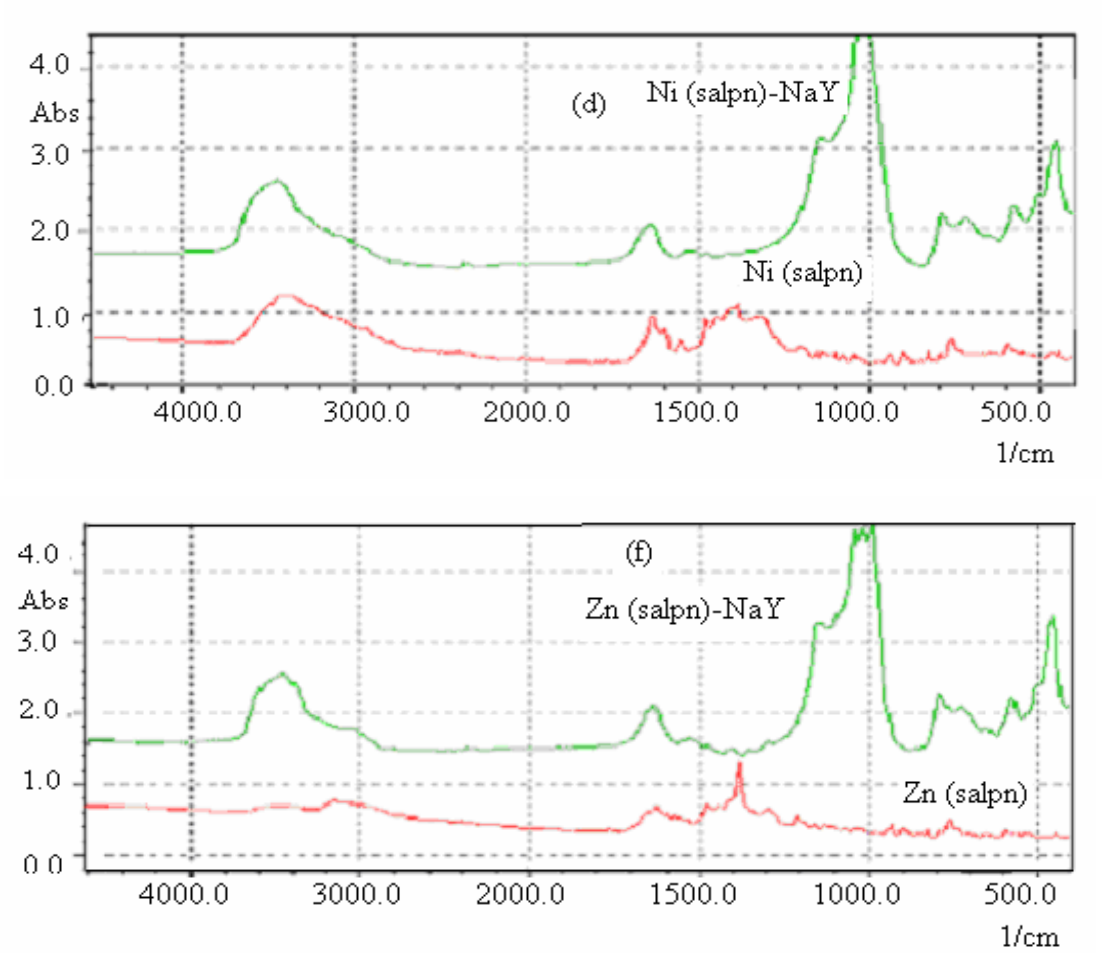

Figure 7.4 (cont.)

The IR spectra of the encapsulated complexes were essentially similar to that of the free complexes; this was observed from Figure 7.4. However, some IR bands of encapsulated complexes and free ligand showed some differences from each other. For example free ligand (H_2salpn) exhibited ν(C=N) stretch at 1580 1/cm. In complexes, this band shifted to lower frequency. As seen in Table 7.2, this band appeared in the range 1523-1570 1/cm. This shift was the indication of the coordination of azomethine nitrogen to the metal. Our results showed good agreement with the results reported in the literature earlier (Maurya et al. 2002a; Maurya et al. 2003). According to the FTIR results, there was no significant expansion of the zeolite cavities, dealumination or structural changes during the encapsulation process. IR spectra of NaY zeolite, metal-exchanged zeolites and catalysts were shown in Figure 7.3. This indicated that, the structure of metal complexes fitted nicely within the cavity of the zeolite. The presence of several bands of low intensity in 2700–2900 1/cm regions indicated the existence of ethylene group of the amine residue of the ligand.

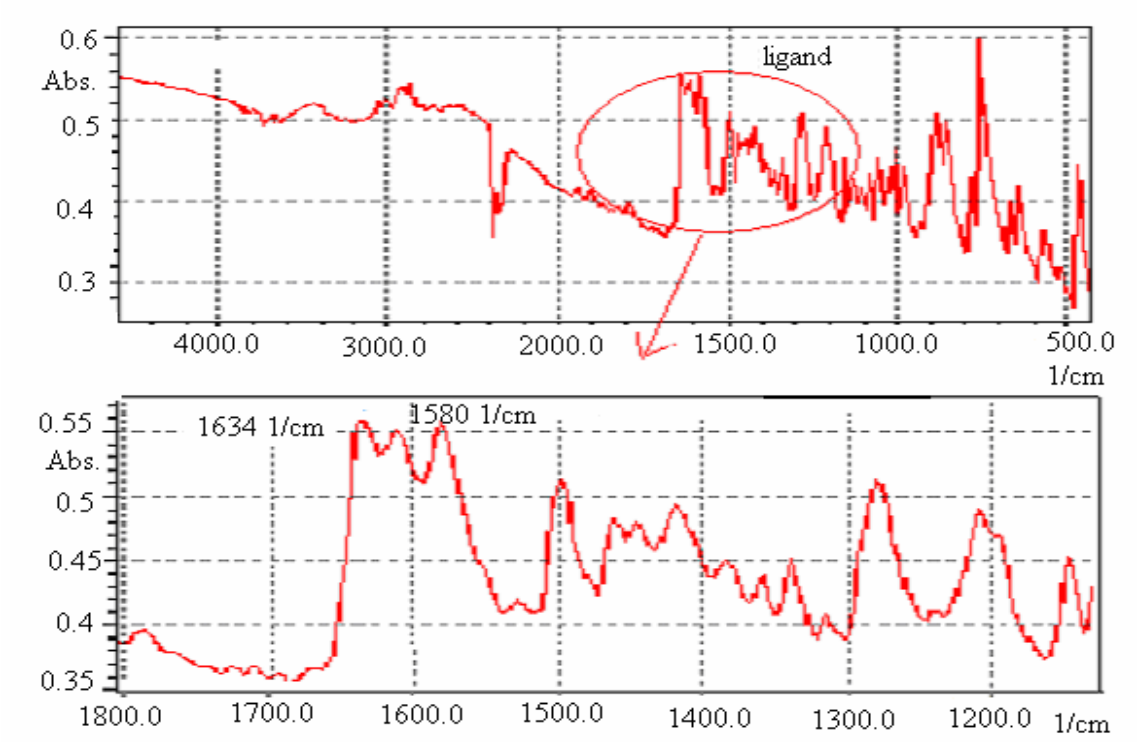

Figure 7.5. IR spectra ligand (H_2 salpn)

Table 7.2. IR spectral data of ligand, its neat and encapsulated complexes

Compound	IR (1/cm)	
	νC=N	νC=C
H_2 (salpn)	1580	1634
Cr(salpn)-NaY	1525	1626
Cr(salpn)	1531	1616
Fe(salpn)-NaY	1545	1635
Fe(salpn)	1570	1624
Bi(salpn)-NaY	1523	1638
Bi(salpn)	1570	1635
Ni(salpn)-NaY	1523	1639
Ni(salpn)	1546	1632
Zn(salpn)-NaY	1525	1640
Zn(salpn)	1554	1627

7.1.5. Pore Volume and Surface Area Measurement

The specific surface areas of the adsorbents can be determined by applying the Langmuir model equation for Type I isotherm. Nitrogen physisorption isotherms of NaY zeolite, Cr NaY and Cr (salpn)-NaY were obtained. They were Type I isotherms according to IUPAC classification. The micropore volume and size reduced apparently after modification also indicated that the metal complex was successfully introduced into the inner channels of Cr based catalyst. The results were summarized in detail in Table 7.3.

Table 7.3. Surface area and micropore volume analysis

Materials	Langmuir surface area (m^2/g)	Micropore volume (cm^3/g) (from Horvath-Kawazoe)
NaY zeolite	807	0.34
Cr NaY	801	0.27
Cr(salpn)-NaY	536	0.22

Surface areas were found to be between 536 and 807 m^2/g as seen in Table 7.3. The Horvath-Kawazoe method can be applied for a quantitative determination of the micropore volume. In the literature, it was frequently reported that the lowering the pore volume and surface area was the indication the metal complexes were present within the zeolite cages (Varkey et al. 1998, Joseph et al. 2002).

7.1.6. Thermal Analyses

7.1.6.1. Differential Scanning Calorimetric Analysis of Ligand

The melting point of ligand (H_2 salpn) was found by differential scanning calorimetric analysis (DSC). Melting point of ligand was found as 53 ºC ($\Delta H = -73.54$ kJ/kg) by differential scanning calorimetric (DSC) analysis as seen in

Figure 7.6. DSC analysis result showed good agreement with previously reported melting point value of 52 ºC (Maurya et al. 2002a).

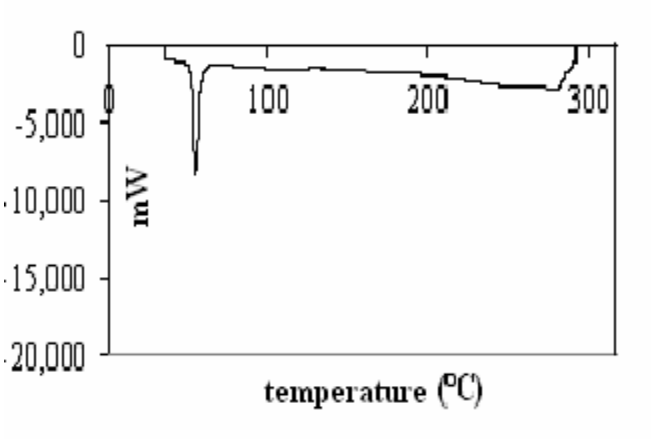

Figure 7.6. DSC analysis of H_2 (salpn) (L) ligand

7.1.6.2. Thermal Gravimetric Analyses (TGA)

TGA curves of the NaY zeolite, Cr exchanged NaY zeolite, Cr (salpn)-NaY catalysts were shown in Figure 7.7. Total amount of water lost below 800^o C in each sample was represented in Table 7.4.

Table 7.4. Total amount of weight loss up to 800 ^{o}C for NaY, CrNaY, Cr(salpn)-NaY

Sample	**% Weight loss up to 800 ^{o}C**
NaY	23.7
CrNaY	24.1
Cr (Salpn)-NaY	25.5

TGA analysis of NaY, Cr exchanged NaY zeolite shows that there was a total mass decrease of 23.7%, 24.1%, which can be attributed to dehydration (Chavan et al. 2000). Cr (salpn)-NaY presented a total mass decrease of 25.5%, due to the loss of water and organic material. The water loss values between 23.7% and 24.1% for NaY zeolite and CrNaY indicated the dependence of water content of zeolite Y on the cation type. When Cr ion was exchanged with Na ion, the water containing of zeolite was changed.

Two stages of weight losses were observed for Cr (salpn)-NaY catalyst up to 510 ºC. The weight losses of %14.8 in the temperature range 30-258 ºC corresponds to the physically adsorbed and chemisorbed (in the form of OH groups) intra-zeolite water in the zeolite channels and cavities as well as the water coordinated to Cr (salpn) complex. Other stage of smaller weight losses (% 9.7) in the temperature range 260-470 ºC was observed. This loss occurs in the wide temperature range and it was due to the slow decomposition of ligand. A smaller weight percentage loss indicates the insertion of only small amount of metal complexes in the zeolite NaY cavities (Maurya et al. 2002a). This was an agreement with low percentage of metal content estimated by inductively coupled plasma (ICP) technique.

Both TGA and pore volume and surface area measurements techniques supported encapsulation of Cr (salpn) complex.

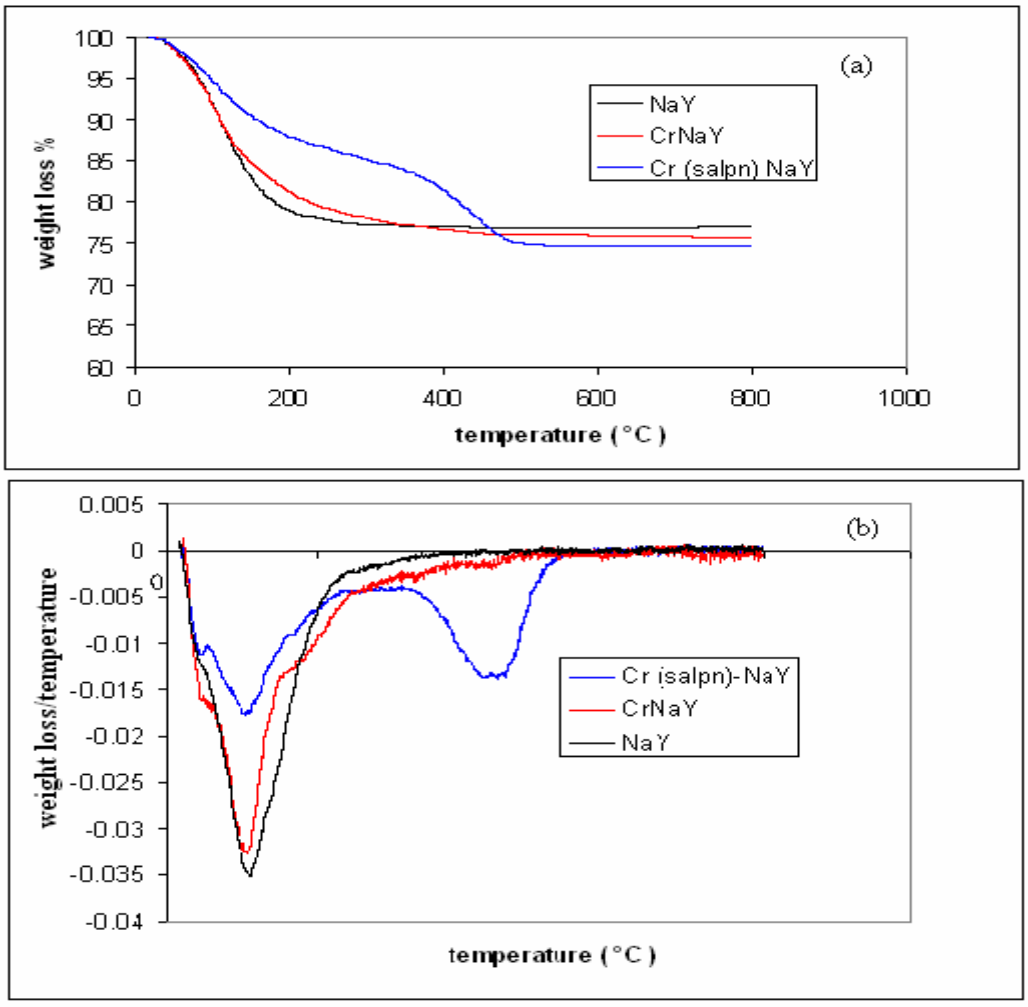

Figure 7.7. TGA (a) and DT/TGA (b) curves of the NaY, CrNaY and Cr (salpn)-NaY catalyst

7.2. Catalytic Activities

7.2.1. Decomposition of H_2O_2

Decomposition of hydrogen peroxide was performed over prepared catalysts for their catalytic activities. The percentage decomposition of hydrogen was measured at two different reaction times (1 hour and 2 hours) and relevant data were presented in Table 7.5. The results showed that the decomposition of hydrogen peroxide after 1 hour was relatively slow (1.2-5.9%) for Fe, Zn, Bi and Ni based catalysts, while Cr based catalyst showed decomposition of 10.4%. Hydrogen peroxide decomposition rate was higher for Cr(salpn)-Y, Fe(salpn)-Y catalysts compared to others. The decomposition of hydrogen peroxide increased for all catalysts even after 2 hours. Cr(salpn)-NaY catalyst was highly active for the hydrogen peroxide decomposition. According to the Table 7.5, Fe(salpn)-NaY, Cr(salpn)-NaY, Bi(salpn)-NaY catalysts continued to decompose hydrogen peroxide significantly even after 2 hours. In the presence of available hydrogen peroxide, Cr(salpn)-NaY, Fe(salpn)-NaY catalysts were able to decompose hydrogen peroxide effectively and they were expected to have higher activities towards the oxidation of carvacrol compared to the other catalysts. The calculation procedure of percentage decomposition of hydrogen peroxide was shown in Appendix A.

Table 7.5. Percentage decomposition of hydrogen peroxide after 1 hour and 2 hours of contact time at ambient temperature

Catalyst	Percentage H_2O_2 reacted (1h)	Percentage H_2O_2 reacted (2h)
Cr(salpn)-NaY	10.4	27.7
Fe(salpn)-NaY	5.9	11.4
Bi(salpn)-NaY	1.8	10.4
Ni(salpn)-NaY	1.2	4.5
Zn(salpn)-NaY	3.2	5.8

7.2.2. Oxidation of Carvacrol

Catalytic activities of prepared catalysts were evaluated for the oxidation of carvacrol with hydrogen peroxide by using HPLC analysis technique. Table 7.6 summarizes the results i.e., percentage of carvacrol conversion and products formed along with their yield. Yield and conversion values were determined from carvacrol and thymoquinone calibration curves which were shown in Appendix B. It was known that encapsulation of metal ions in zeolites could result in unusual oxidation states/electronic configurations and consequent catalytic activity. Hydrogen peroxide has advantage of high mobility in the pores of zeolite system due to its smaller size. Moreover hydrogen peroxide is cheaper and sufficiently environment-friendly. Hydrogen peroxide alone was unable to oxidize carvacrol to a significant extent. With NaY zeolite, no significant carvacrol oxidation reactions were investigated in this study, indicating that Y zeolite was inactive under the reaction conditions (Table 7.6). Oxidation of carvacrol cannot occur unless a catalyst promotes the reaction. This observation was in agreement with the observations made by several researchers (Skrobot et al. 2003; Xavier et al. 2004). To determine the performance of the catalysts, the percentage of carvacrol conversion was plotted as a function of time at two different carvacrol-to-hydrogen peroxide molar ratios. The results of carvacrol oxidation reactions at carvacrol-to-hydrogen peroxide molar ratios of 3 and 1 were seen in Figures 7.8 and 7.9, respectively. As seen from these figures all catalysts have shown activity for the oxidation of carvacrol.

The catalytic oxidation of carvacrol was expected to give mixture of benzoquinones (Santos et al. 2003) as shown by Eq. (7.1). According to the literature, the quinone may result from the oxidation of a hydroquinone intermediate (Martin et al. 1999, Milos et al. 2001, Santos et al. 2003, Martin et al. 2001). The formation of TQ from carvacrol was a result of the selective hydroxylation of the aromatic ring in the *para* position relatively to the OH group, followed by the subsequent oxidation of the resulting hydroquinone to the quinone stage. This hydroquinone derivative might arise from a protonated intermediate, the *p*-hydroxylated species. Such intermediate was stabilized by the OH present in the carvacrol (Eq 7.1) (Martin et al. 1999).

For the catalytic systems investigated here thymoquinone (TQ), thymohydroquinone (THQ) and other benzoquinones (BQ) appeared successively as

reaction products, among which TQ was predominant. No attempts were made to identify benzoquinones separately.

At carvacrol-to-hydrogen peroxide molar ratio of 3 carvacrol conversion of 11.0%, 7.9% and 3.2% were determined for Zn(salpn)-NaY, Ni(salpn)-NaY and Bi(salpn)-NaY catalysts with close to 100% selectivity, respectively (Table 7.6). In spite of the low carvacrol conversion, the Bi, Ni and Zn based catalysts gave approximately 100% selectivity for the thymoquinone formation (Figure 7.10). Minor products (THQ and BQ) were detected higher conversions as shown in Figure 7.10. Among the prepared catalysts, Cr(salpn)-NaY performed best and gave the highest carvacrol conversion of 14.2%, whereas, Fe(salpn)-NaY recorded carvacrol conversion of 12.7%. In terms of the formation of thymoquinone, a maximum of 13.0% thymoquinone formation was obtained with Cr based catalyst, which was followed by Fe, Zn, Ni and Bi based catalysts in decreasing order.

Table 7.6. Conversion and yield in the oxidation of carvacrol reactions[a]

Catalyst	Carvacrol/H_2O_2 (Molar ratio)	Carvacrol Conversion[b] (%)	Thymoquinone Yield[b] %
Cr(salpn)-NaY	3	14.2	13.0
Fe(salpn)-NaY	3	12.7	11.6
Bi(salpn)-NaY	3	3.2	3.2
Zn(salpn)-NaY	3	11.0	11.0
Ni(salpn)-NaY	3	7.9	7.9
Cr(salpn)-NaY	1	23.5	17.6
Fe(salpn)-NaY	1	27.6	22.0
Bi(salpn)-NaY	1	4.9	4.9
Zn(salpn)-NaY	1	6.7	6.7
Ni(salpn)-NaY	1	5.9	5.9
NaY	1	No detectable activity[c]	

[a] Reaction conditions: Acetonitrile as solvent, 60 ºC, 5 hours, 0.1g catalyst

[b] Conversion, yield were determined by HPLC Conversion of reactant can be calculated as $\left(\frac{(\text{reactant})_{\text{in}} - (\text{reactant})_{\text{out}}}{(\text{reactant})_{\text{in}}}\right) x100$, Yield for a specific product can be calculated as $\left(\frac{\text{product}}{(\text{reactant})_{\text{in}}}\right) x100$

[c] NaY showed no catalytic activity towards oxidation of carvacrol

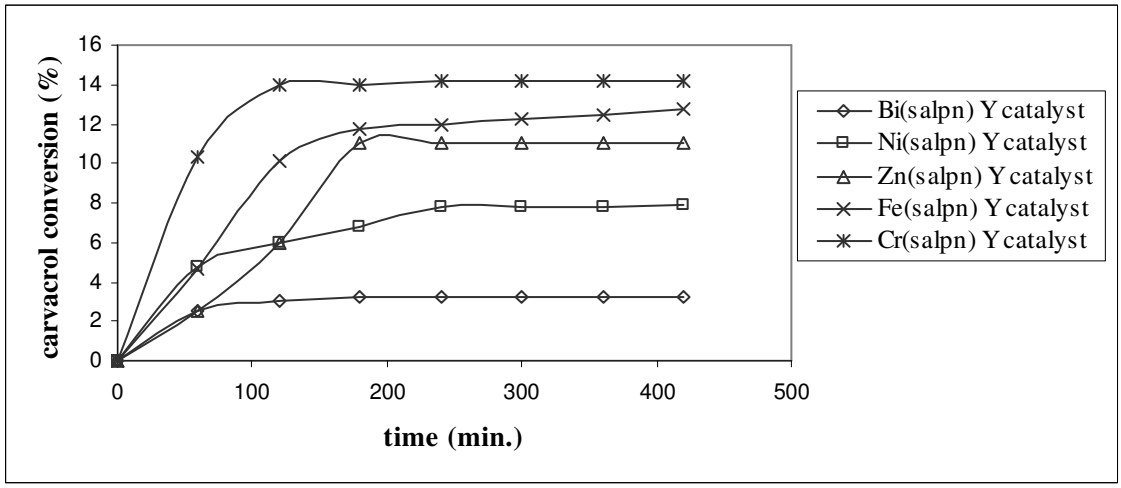

Figure 7.8. The percentage of carvacrol conversion (reaction conditions: carvacrol/H_2O_2 molar ratio=3, 0.1 g catalyst, 60 ºC)

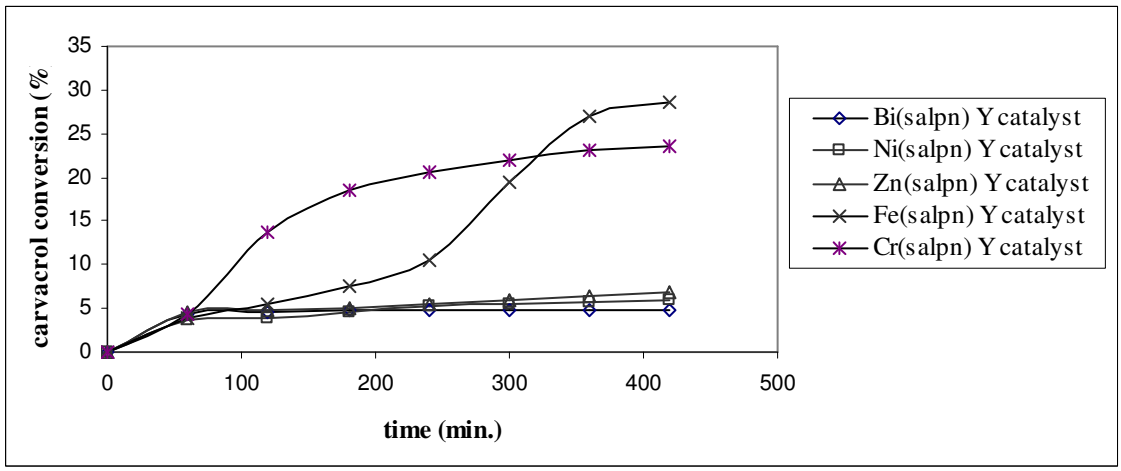

Figure 7.9. The percentage of carvacrol conversion (reaction conditions: carvacrol/H_2O_2 molar ratio=1, 0.1 g catalyst, 60 ºC)

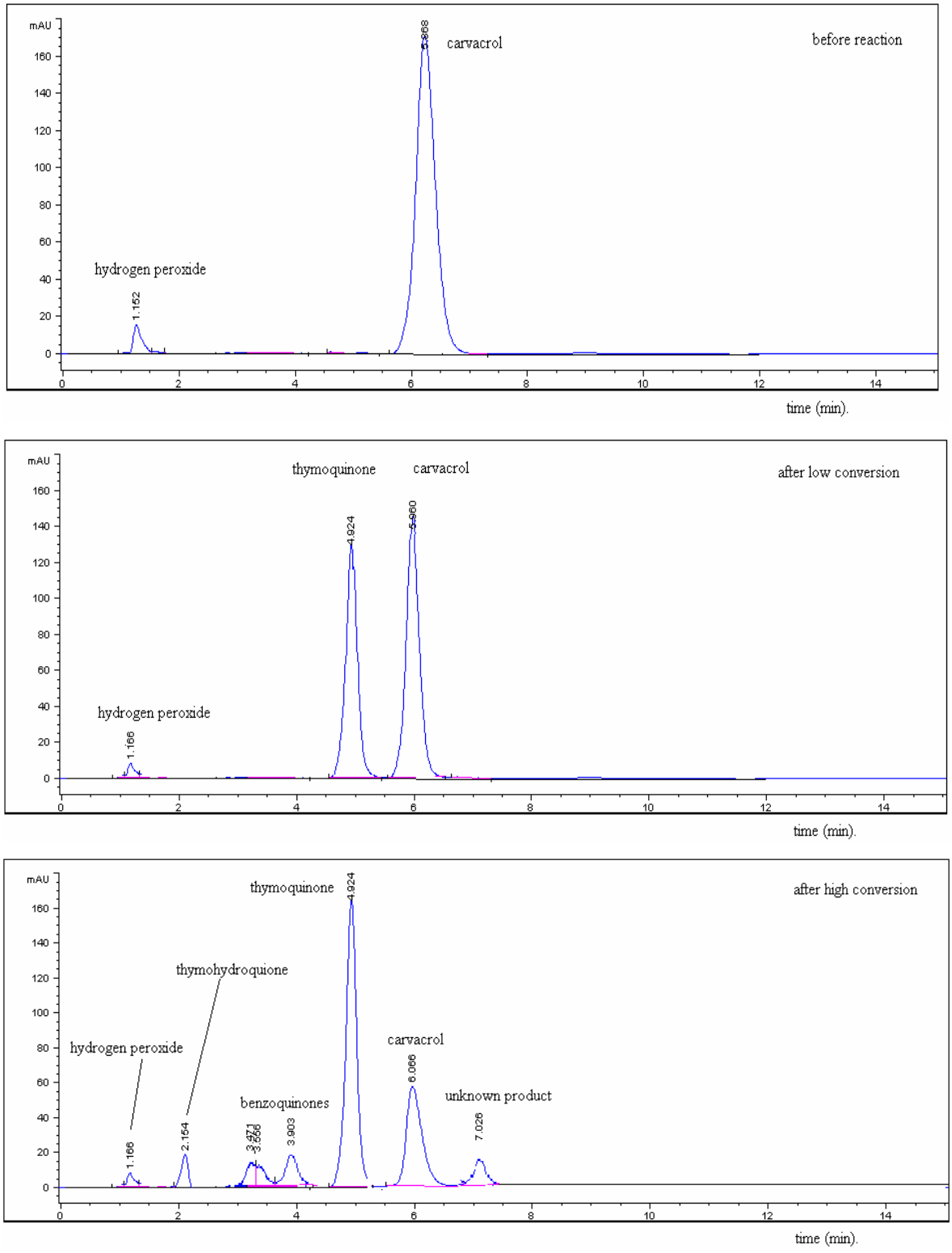

Figure 7.10. Typical HPLC chromatograms of oxidation of carvacrol reaction recorded for before and after for low and high conversions

With Cr-based catalyst 13% of TQ was observed along with small amounts of THQ and BQ. On the other hand, using Fe-based catalyst, TQ formation was found to

be 11.6% with a small amount of THQ. Zn, Ni and Bi catalysts were more selective for the TQ formation compared to Fe and Cr based catalysts. However, the leached metal ions detected by ICP technique in the reaction medium catalyzed the carvacrol oxidation reaction homogeneously. Therefore, it was difficult to call these catalysts as complete heterogeneous catalysts due to significant metal ion leaching from catalysts to reaction medium. For Zn, Ni and Bi, Fe, catalysts the presence of metal ions in the reaction mixture after 5 hours was detected by ICP analysis. The percentage of leached metal ions to the reaction medium was 25.2%, 19%, 64%, 10% for Zn, Ni and Bi, Fe catalysts respectively (reaction conditions: carvacrol/H_2O_2 molar ratio=3, 0.1 g catalyst, 60 ºC). For Cr catalyst no metal ion was detected by ICP technique. Since Cr and Fe-based catalysts have shown better catalytic activity than the others we decided to examine the heterogeneities of these catalysts (in section 7.2.3) by hot filtration technique further and the results were presented later in the text. As seen from Figure 7.8 conversion of carvacrol increased with time for all catalysts, but reached a steady state at different times. The maximum conversion of about 14.2% was observed with Cr(salpn)-NaY after a period of 1.5 hours. For Fe(salpn)-NaY 12.7% carvacrol conversion was observed within 2 hours. Rest of the catalysts recorded lower conversions than Fe(salpn)-NaY, Cr(salpn)-NaY catalysts.

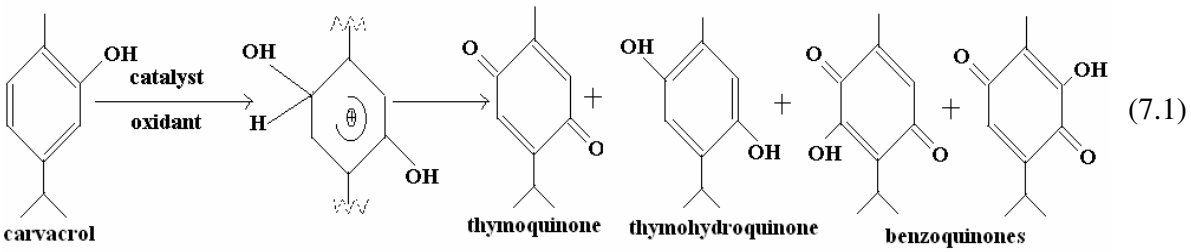

(7.1)

As seen from Table 7.6, maximum conversions were achieved by using Cr(salpn)-NaY and Fe(salpn)-NaY catalyst for both carvacrol-to-hydrogen peroxide molar ratios of 3 and 1. When the carvacrol-to-hydrogen peroxide molar ratio was decreased to 1 (i.e.; increasing hydrogen peroxide) again, the oxidation of carvacrol gave thymoquinone with close to 100% selectivity for Zn, Ni and Bi catalysts. The selectivity towards thymoquinone decreased with increasing carvacrol conversion for Fe(salpn)-NaY and Cr(salpn)-NaY catalysts. The decrease in selectivity was due to the two more components observed in the reaction mixture and no attempts were made to identify them. Some of them were probably higher molecular weight compounds

forming in the reaction mixture due to the association of thymoquinone, as thymoquinone has a tendency to polymerize.

For Fe(salpn)-NaY catalyst, carvacrol conversion increased much higher than the other catalysts as seen in Figure 7.9. This increase in carvacrol conversion could be explained by hydrogen peroxide decomposition data. According to this data, Fe(salpn)-NaY catalyst reached equilibrium in a longer time. Fe-based catalyst has shown a good activity and carvacrol conversion increased from 12.7% to 27.6% after increasing the hydrogen peroxide amount. Reaction continued with more available hydrogen peroxide. Carvacrol conversion increased from 14.2% to 23.5% for Cr(salpn)-NaY catalyst after increasing the hydrogen peroxide amount. The Zn and Ni-based catalysts, except Bi based catalyst (4.9%), have shown smaller conversion values of 6.75% and 5.9%, respectively compared to when carvacrol-to-hydrogen peroxide ratio was 3.

In the literature, the oxidation of carvacrol with hydrogen peroxide was studied by using Mn(III) porphyrin complexes (Martin et al. 1999). Fe(III) meso-tetraphenylporphyrin or Fe(III) phthalocyanines (Milos et al. 2001) and keggin-type tungstoborates (Santos et al. 2003) under homogeneous conditions. Mn(III) porphyrin complexes showed high carvacrol conversion with a selectivity range 70-99.6%. Oregano essential oil containing mainly 47.6% thymol and 25.1% carvacrol were transformed to oil containing thymoquinone (20-66%) using Fe(III) meso-tetraphenylporphyrin or Fe(III) phthalocyanines complexes (Milos et al. 2001). Keggin-type tungstoborates showed carvacrol conversion values of 35-40% providing mainly mixtures of benzoquinones, with a small amount (2.5%) of TQ (Santos et al. 2003). With heterogeneous catalyst which was zeolite encapsulated Mn(III) tetra porphyrin complexes, the oxidation of carvacrol (<25% conversion) formed thymoquinone with 100% selectivity. However, leaching of the porphyrin from Mn(III)porphyrin-NaY and changes in its crystalline structure occurred (Skrobot et al. 2003).

7.2.3. Heterogeneity Test

To test if the metal complex was leaching out from the catalyst, the reaction mixture was filtered hot. The leaching of the active species from the heterogeneous catalysts into the solution was an important question in order to identify whether the reaction takes place homogeneously or heterogeneously. The catalysts were filtered off

during the oxidation process and the carvacrol was monitored in the filtrate by HPLC. This test was performed only for Cr(salpn)-NaY and Fe(salpn)-NaY catalysts which showed good carvacrol oxidation performance. Times vs. conversion curves with catalyst and after filtrating catalysts were presented in Figure 7.11.

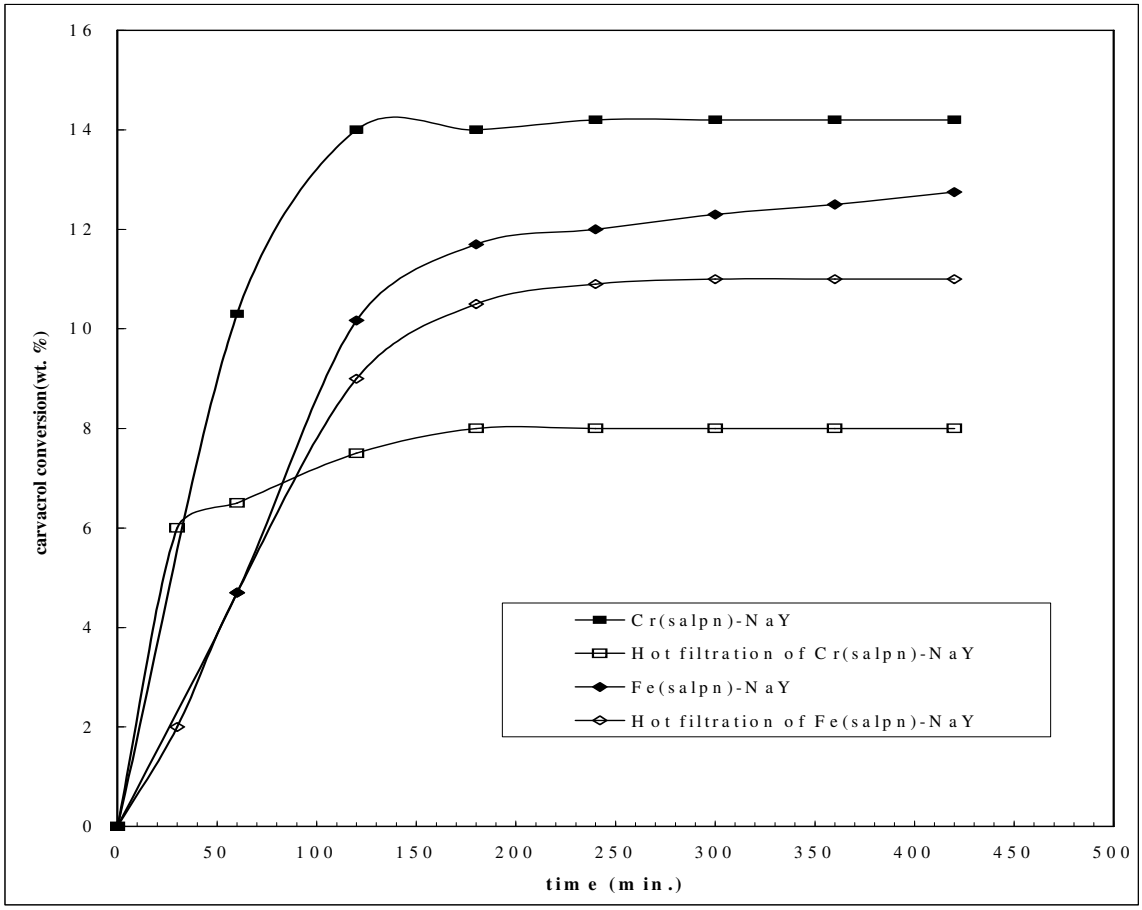

Figure 7.11. The percentage of carvacrol conversion (reaction conditions: carvacrol/ H_2O_2 molar ratio=3, 0.1 g catalyst, 60 ºC, hot filtration at 30 minutes)

No further reaction was noted after the catalyst removal for the Cr(salpn)-NaY as seen in Figure 7.11. However, when Fe(salpn)-NaY catalyst was removed from the reaction mixture the carvacrol conversion decreased but continued. It was clear that heterogeneity of Cr-based catalyst was better than Fe-based catalyst. Carvacrol/hydrogen peroxide molar ratios 1 and 3 were tested for leaching test at 60 ºC with 0.1 g catalyst. No any significant differences were observed for Cr (salpn)-NaY catalyst and Fe (salpn)-NaY catalyst. The chromium complex when immobilized seemed to be more stable than the iron complex in the oxidizing medium

The average size of Cr (salpn) complex was about 12.7 Å which was determined from spartan program (Wavefunction, Inc.1996-1997, trial version) as shown in Figure 7.12. Before complexation, the size of ligand was about 7 Å. It shows clearly this complex was too large to diffuse out from the zeolite cage. Size of other metal complexes were between 8-10 Å. Their size were nearly the same with zeolite channel so they can diffuse out more easier than Cr(salpn) complex. This easiness of diffusion also confirmed by ICP and heterogeneity results.

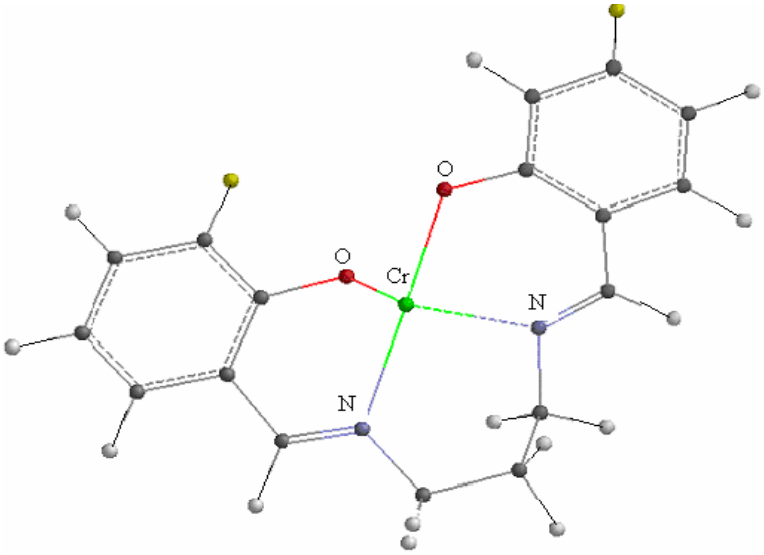

Figure 7.12. Cr (salpn) complex.

7.2.4. Cr (salpn)-NaY Catalyst Recycle

A salient advantage of heterogeneous catalysts is the ease with which they are separated from the reaction products. Separated heterogeneous catalysts should be reused in reactions.

So in this thesis study, the used Cr (salpn)-NaY catalyst was used under the same reaction conditions as for the initial run (reaction conditions: carvacrol/H_2O_2 molar ratio=3, 0.1 g Cr (salpn)-NaY catalyst, 60 ^oC). Then the catalyst was filtrated at the end of the each reaction and washed with acetonitrile, dried at 50 ^oC. The dried catalyst was used at the same reaction condition. At the end of fourth reaction, carvacrol conversion decreased from 14.2% to 3% as shown in Figure 7.13.

Although recycling property is so important parameter for heterogeneous catalyst system. Cr (salpn)-NaY catalyst may be recycled for two or three times. There was a progressive loss of activity with lowering in carvacrol conversion indicating

leaching of Cr (salpn) complexes from the catalyst. This was also confirmed by visible gradual change in color of the catalyst surface for every cycle. Slow leaching of metal was observed over reuse which can limit their application and needs further investigation.

As seen in Figure 7.13, for second recycle carvacrol conversion did not change significantly. This can be explained by checking Figure 7.11, after hot filtration of catalysts carvacrol conversion did not increase significantly. For first recycle of catalyst, no leaching of Cr metal ions was observed. So, deactivation or leaching of metal ions was observed after the second recycle.

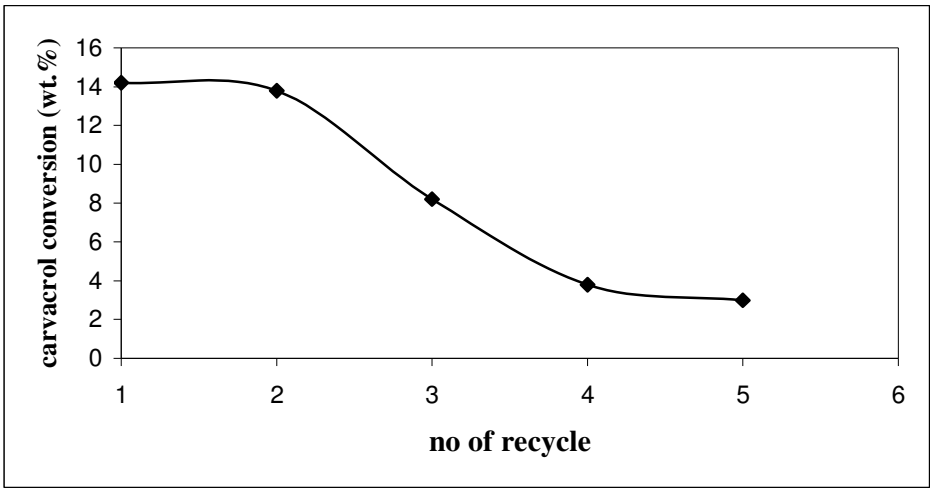

Figure 7.13. Carvacrol conversion (wt. %) vs number of recycle

As a result of all of these studies, Cr (salpn)-NaY catalyst was found to be a more efficient catalyst than other catalysts based on catalyst activity and leaching tests. With this catalyst, some parameters effects on carvacrol oxidation reaction were investigated.

7.3. Effect of Parameters for Carvacrol Oxidation Reactions with Selected Cr (Salpn)-NaY Catalyst

In order to determine the effect of various reaction parameters such as catalyst amount, temperature, reactant/H_2O_2 molar ratio on the catalytic performance, oxidation of carvacrol was carried out using Cr (salpn)-NaY catalyst. The low, intermediate and high values were presented in Table 7.7.

Table 7.7. Values of parameters

	low value	intermediate value	high value
temperature (ºC)	40	50	60
carvacrol / (%30)H_2O_2 (molar ratio)	1	2	3
4.5 ml carvacrol (constant)	3ml (%30)H_2O_2	1.5ml (%30)H_2O_2	1ml (%30) H_2O_2
catalyst amount (g)	0.05	0.13	0.2

[a] Reaction conditions: Acetonitrile as solvent, 5 hours reaction time

7.3.1. Effect of Catalyst Amount

The effect of catalyst amount on the carvacrol oxidation reaction was given in Table 7.8. From the table, it was clear that by using 0.05 g catalyst at 50 ºC with a molar ratio of 2 only 7.4% carvacrol conversion was obtained. An increasing amount of catalyst weight from 0.05g to 0.13g or 0.2g has enhanced performance. Increment of catalyst amount hardly improved the conversion. Increase in carvacrol conversion while increasing catalyst amount indicates of reaction was catalytic in nature. This result was also observed in phenol oxidation reactions (Maurya et al. 2003). In phenol oxidation reaction, up to certain catalyst weight conversion was increased then no significant increasing was observed. This can be explained by the saturation of active sites and this was probably due to more rapid hydrogen peroxide decomposition at large catalyst amount. When conversion increased with increasing catalyst amount higher amount TQ was observed with small amount of THQ and BQ derivatives. With low catalyst amount, reactions were more selective for TQ formation compared to higher catalyst amount.

7.3.2. Effect of Temperature

Four different temperatures (25, 40, 50, 60 ºC) were used while keeping other parameters fixed (i.e. catalyst weight, carvacrol / (%30) H_2O_2 (molar ratio)). The results were presented in Table 7.8. At 60 ºC reaction temperature, high conversion (19.2 %) was observed. At low temperature value 25 ºC, no carvacrol conversion was observed. With the same catalyst, in phenol oxidation reactions at least 50 ºC was required temperature to obtain a conversion (Maurya et al. 2002, Maurya et al. 2003). At 50, 60 ºC, 16, 15% TQ was observed with small amount of THQ and BQ derivatives. At low temperatures reactions were more selective for TQ formation compared to high temperatures. However, in these reactions conversions were low (i.e. 6.2%).

7.3.3. Effect of carvacrol/(%30) H_2O_2 (molar ratio)

The effect of hydrogen peroxide concentration on percentage carvacrol conversion as a function of reaction time has been also studied. The carvacrol / (%30) H_2O_2 (molar ratio) used were 1, 2, 3 while the amount of carvacrol was kept constant with other parameters. The percentage of carvacrol conversion has been found to increase with the decreasing carvacrol/(%30) H_2O_2 (molar ratio) in other words increasing H_2O_2 amount (Table 7.8). However by increasing the H_2O_2 amount the system was attained a steady state after a certain time. This result showed good agreement with previously reported hydrogen peroxide effect on oxidation reactions (Maurya et al. 2002). When conversion increased by decreasing carvacrol / (%30) H_2O_2 (molar ratio) in other words increasing H_2O_2 amount; higher TQ (23%) amount was observed with small amount of THQ and BQ derivatives. For lower conversions, reactions were more selective for TQ formation compared to higher conversions.

Table 7.8. Oxidation of carvacrol by Cr (salpn)- NaY catalyst under different reaction conditions[a]

catalyst amount (g)	temperature (^oC)	carvacrol / (%30)H_2O_2 molar ratio	Conversion[b] (%)	TQ yield[b] (%)
effect of catalyst weight				
0.05	50	2	7.4	7.4
0.13	50	2	18.0	16.0
0.2	50	2	21.6	20.7
effect of temperature				
0.13	25	2	no conversion	-
0.13	40	2	6.2	6.2
0.13	50	2	18.0	16.0
0.13	60	2	19.2	15.0
effect of H_2O_2 amount				
0.13	50	3	3.7	3.7
0.13	50	2	18.0	16.0
0.13	50	1	27.0	23.0

[a] Reaction conditions: Acetonitrile as solvent, 5 hours reaction time, Cr (salpn)-NaY catalyst was used

[b] Conversion, yield were determined by HPLC. Conversion of reactant can be calculated as $\left(\frac{(\text{reactant})_{in} - (\text{reactant})_{out}}{(\text{reactant})_{in}}\right) x100$, Yield for a specific product can be calculated as $\left(\frac{\text{product}}{(\text{reactant})_{in}}\right) x100$

7.4. Oxidation of Thymol

Carvacrol and Thymol are aromatic monoterpenes, which can be found in the essential oils of many aromatic plants. They are geometrical isomers. Their chemical structures are very similar as seen in Figure 7.14 (Martin et al. 1999).

(a) **(b)**

Figure 7.14. Structure of (a) Thymol and (b) Carvacrol (Milos et al. 2001).

From the leaching (heterogeneity test) results and catalyst activity tests for carvacrol conversion reactions, Cr (salpn)-NaY was found to be relatively more efficient and stable catalyst than the others. So thymol oxidation and essential oil oxidation reactions were carried out with Cr (salpn)-NaY catalyst.

The conversion of carvacrol and thymol values was in the 35-39% range. Their conversion vs time profiles given in Figure 7.15 were very similar because of similarities between their structures. Oxidation of carvacrol and thymol provided mainly mixture of TQ, THQ and BQ with a 31.2%, 34.5% TQ yield respectively. The yields of thymol and carvacrol were very close to each other.

In literature, TQ was produced only in small amount as a result of carvacrol and thymol oxidation reactions by using different type of catalyst (Santos et al. 2003). However in our study, a relatively higher TQ formation was yielded for both thymol and carvacrol oxidation reactions.

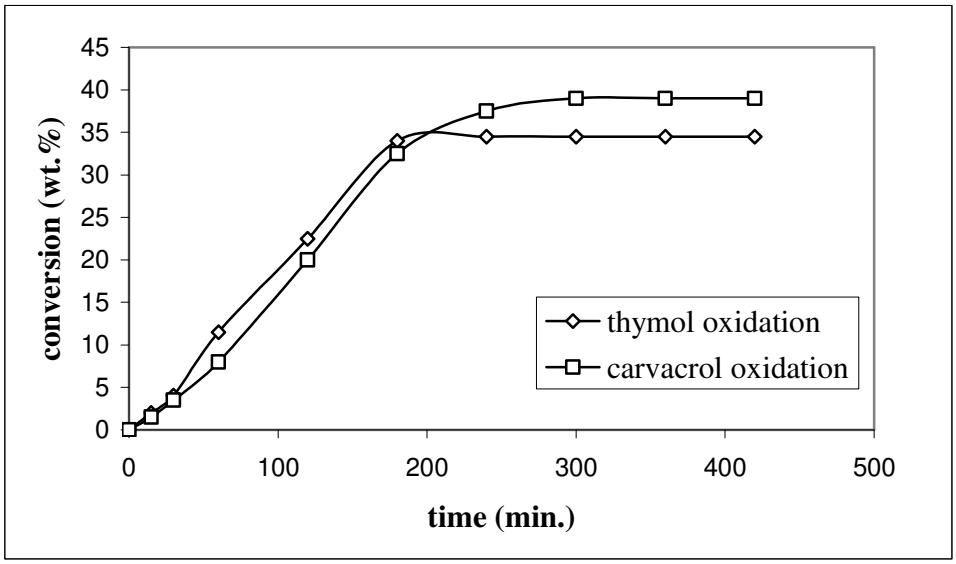

Figure 7.15. The percentage of thymol and carvacrol conversion (reaction conditions: thymol or carvacrol/H_2O_2 molar ratio=1, 0.2 g Cr (salpn)-NaY catalyst, 60ºC)

7.5. Oxidation of Thyme Essential Oil

There were several reports in the literature about the chemical composition of essential oil. The summary of these studies were also given in Chapter 5. Most reports indicated that thymol or carvacrol were the major component in the essential oil (Dorman et al. 1995). In this study, essential oil which was purchased from Arifoğulları Company was analyzed in HPLC.

Essentail oil contains many monoterpenes. However, in HPLC analyses only carvacrol and thymoquinone were observed and no other components were identified such as thymol, p-cymene, α-terpinene for three different wavelengths (254 nm, 280 nm, 295 nm).

In the literature for oxidation reactions, large differences have been observed between GC and HPLC analysis results. Using GC for the analysis of reaction mixtures in the presence of residual H_2O_2, products were oxidized by H_2O_2 at elevated temperature in the GC system (Ma et al. 2002). Hence, lately HPLC was preferred technique for the oxidation reactions.

As shown in Figure 7.16 carvacrol was the major component and it was converted to BQ, THQ, TQ (with 33.6% yield), unknown products with 70% conversion

at 60 °C. Essentail oil contained thymoquinone. After the oxidation reaction thymoquinone amount was increased.

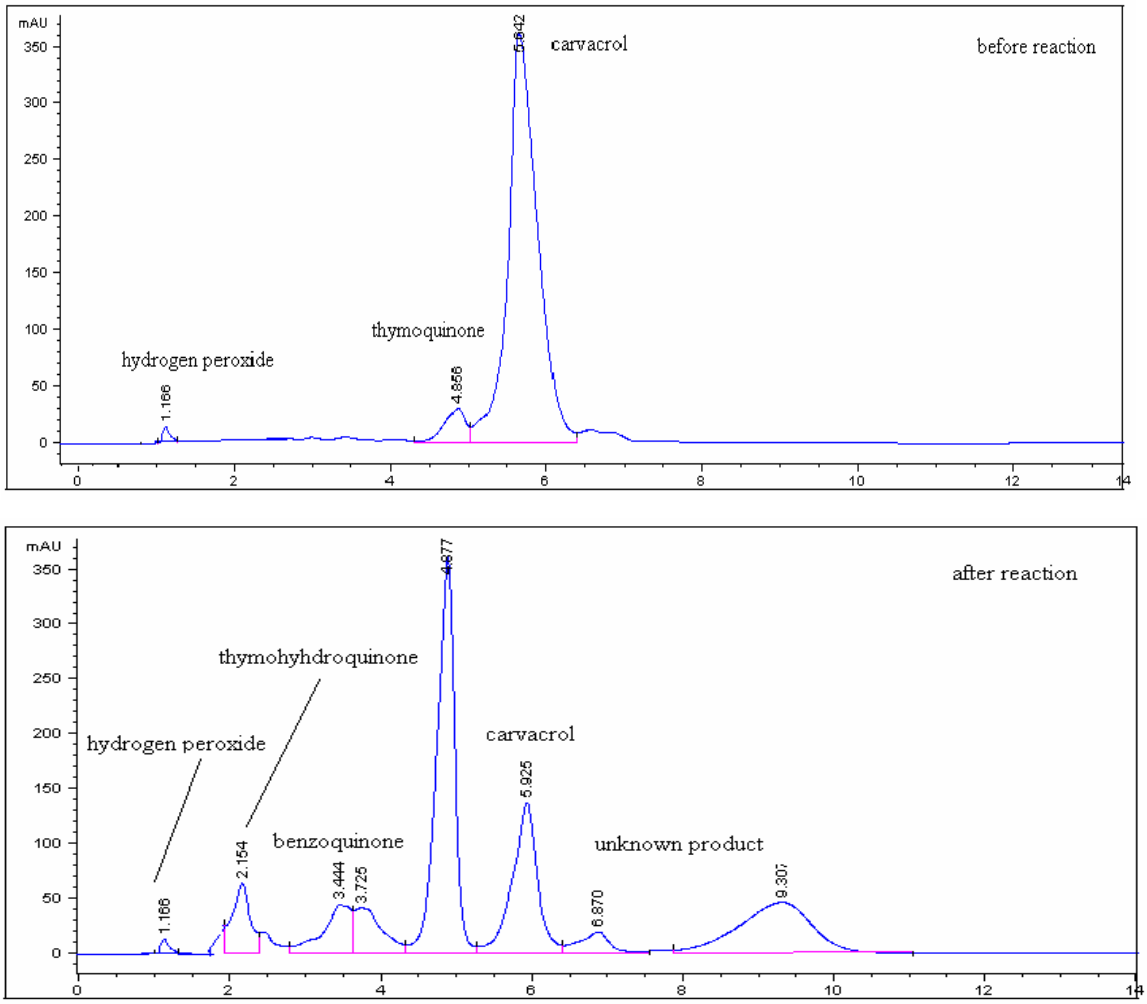

Figure 7.16. HPLC chromatograms of thyme essential oil before and after oxidation reaction (reaction conditions: 0.2 g Cr (salpn)-NaY catalyst, 60 ºC)

CHAPTER 8

CONCLUSION

NaY zeolite-encapsulated Ni (II), Zn(II), Bi(III), Fe(III) and Cr(III) complexes of H_2salpn ligand have been prepared using flexible ligand method. The characterization results obtained by XRD, SEM and FTIR, BET, TGA confirmed the encapsulation of metal complexes in the supercages of NaY zeolite. The all of the NaY zeolite-encapsulated complexes were active catalysts for the decomposition of hydrogen peroxide and for the oxidation of carvacrol.

Thymoquinone, is a compound with a commercial value considerably higher than its precursors (thymol and carvacrol). Thymol and carvacrol found in thyme essential oil. Thymoquinone can be easily obtained by catalytic oxidation of these precursors using environmentally cheap oxidizing agent, hydrogen peroxide and zeolite-encapsulated metal(salpn) complexes as heterogeneous catalysts.

Leaching tests revealed the heterogeneity of the catalysts. However, Cr(salpn)-NaY and Fe(salpn)-NaY catalysts have shown good activity. So heterogeneity test was performed for two catalysts. Cr(salpn)-NaY showed a good performance in terms of activity towards carvacrol oxidation reaction and heterogeneity. With this catalyst, catalyst amount, temperature and carvacrol to hydrogen peroxide molar ratio effects on carvacrol oxidation reaction were investigated. All parameters were found as effective parameters. Increasing the temperature, catalysts amount, hydrogen peroxide amount caused the increasing the yield of thymoquinone and carvacrol conversion.

Thymol and thyme essential oil were oxidized with Cr-(salpn)-NaY catalyst. Thymoquinone yield in carvacrol and thymol oxidation reactions were found to be very close to each other due to the similarities in their chemical structures. After the essential oil oxidation reaction, thymoquinone amount was increased in oil.

REFERENCES

Anthony, F., 1999. *Advances in Organic Chemistry*, (McGraw-Hill, New York), pp. 148-167.

Arends, I.W.C.E., Sheldon R.A. 2001. "Activities and Stabilities of Heterogeneous Catalysts in Selective Liquid Phase Oxidations: Recent Developments", *Applied Catalysis A*: *General*. Vol. 212, pp.175-187.

Armengol, E., Cormo, A., Fornes, V., Garcia, H., Primo, J. 1999. "Cuphthalocyanine and Co Perfuorophthalocyanine Incorporated Inside Y Faujasite and Mesoporous MCM-41 as Heterogeneous Catalysts for the Oxidation of the Cylohexane", *Applied Catalysis A*: *General*. Vol. 181, pp. 305-312.

Badary, O.A. 1999. "Thymoquinone Attenuates Ifosfamide-Induced Fanconi Syndrome in Rats and Enhances its Antitumor Activity in Mice", *Journal of Ethnopharmacology*. Vol. 67, pp.135-142.

Balkus, Jr., Gabrielov, K.J. 1995. "Zeolite Encapsulated Metal Complexes", *Journal of Inclusion Phenomena and Molecular Recognition in Chemistry*. Vol. 21, pp.159-184.

Baydar, H., Sagdic, O., Ozkan, G., Karadogan, T. 2003. "Antibacterial Activity and Composition of Essential Oils from Origanum, Thymbra and Satureja Species with Commercial Importance in Turkey", *Food Control*. Vol.15, pp.169-172.

Bennur, T.H., Srinivas, D., Ratnasamy, P. 2001. "EPR Spectroscopy of Copper and Manganase Complexes Encapsulated in Zeolite", *Microporous and Mesaporous Materials*. Vol. 48, pp.111-118.

Berteli, D., Plessi, M., Miglietta, F. 2003. "Effect of Microwaves on Volatile Compounds in Origanum ", *Lebensm.-Wiss. U.-Technol* . Vol. 36, pp.555–560.

Breck, D.W., 1974. *Zeolite Molecular Sieves*, (John Wiley and Sons, Interscience Publication), pp. 4-5.

Bregeault, J.M. 2003. "Transition Metal Complexes for Liquid Phase Catalytic Oxidation: Some Aspects of Industrial Reactions and of Emerging Technologies", *Dalton Transition*. pp. 3289-3302.

Brunel, D., Bellocq, N., Sutra, P.,Cauvel, A., Laspe´ras, M., Moreau, P., Di Renzo, F., Galarneau, A., Fajula, F. 1998. "Transition-Metal Ligands Bound Onto the Micelle-Templated Silica Surface", *Coordination Chemistry Reviews*. Vol.178–180, pp.1085-1108.

Canbeşer, K.H., Demirci, B., Kirimer, N., Satil, F., Tümen, G. 2002. "The Essential Oils of *Thymus Migricus* and *T. Fedtschenkoi handelii* from Turkey", *Flavour Fragrance Journal*. Vol.17, pp.41-45.

Chandra, R.J., Varkey, S., Ranasamay, P. 1998. "Selective Oxidation Over Copper and Manganese Salens Encapsulated in Zeolites",*Microporous and Mesoporous Materials*. Vol. 22, pp. 465-474.

Chandra, R.J., Varkey, S., Ranasamay, P. 1998. "Zeolite Encapsulated Copper (X_2 Salen) Complexes", *Applied Catalysis A*: *General*. Vol. 168, pp. 353-364.

Chandra, R.J., Varkey, S., Ranasamay, P. 1999. "Oxidation of Para-xylene Over Zeolite-Encapsulated Copper and Manganese Complexes", *Applied Catalysis A*: *General*. Vol. 182, pp. 91-96.

Fan, B., Fan, W., Li, R. 2002. "Fe Containing Y as a Host for the Preparation of a Ship-in-a-bottle Catalyst", *Journal of Molecular Catalysis A*: *Chemical*. Vol.201, pp.137-145.

Ghosheh, O.A., Houdi, A., Crooks, P.A. 1999. "High Performance Liquid. Chromatographic Analysis of the Pharmacologically Active Quinones and Related Compounds in the Oil of Black Seed *(Nigella Sativa L.)* ", *Journal of Pharmaceutical and Biomedical Analysis*. Vol.19, pp.757-762.

Figgis, B.N., 1966. *Introduction to Ligand Fields*, (John Wiley and Sons, USA).

Hoelderich, W.F., Kollmer, F. 2000. "Oxidation Reactions in The Synthesis of Fine and Intermediate Chemicals Using Environmentally Benign Oxidants and Right Reactor System", *Pure Applied Chem*istry. Vol. 72, No. 7, pp. 1273–1287.

Joseph, T., Srinivas, D., Gopinath, C.S., Halligudi, S.B. 2002. "Spectroscopic and Catalytic Activity Studies of VO(Soloph) Complexes Encapsulated Zeolite-Y and Al-MCM-41 Moleculer Sieves", *Catalysis Letters*. Vol. 83, pp. 209-214.

Kaduk, J.A., Faber , J. 1995. "Crystal Structure of Zeolıte Y as a Function of Ion Exchange", *Rıgaku Journal*. Vol. 12**,** No. 2, pp. 18-34.

Karaman, S., Digrak, M., Ravid, U., Ilcim, A. 2001. "Antibacterial and Antifungal Activity of the Essential Oils of *Thymus Revolutus* Celak from Turkey", *Journal of Ethnopharmacology*. Vol. 76, pp.183–186.

Keim, W. 2002. "Role of Ligands in Homogeneous Catalysis Based on Transition Metals", *Institute of Technical Chemistry and Macromolecular Chemistry*. Vol. 51, No. 6, pp. 930-935.

Ma, N., Ma, Z., Yue, Y., Gao, Z. 2002. "Reaction Testing of Phenol Hydroxylation and Cyclohexane Oxidation by Gas Chromatography: Influence of Residual Hydrogen Peroxide", *Journal of Molecular Catalysis A*: *Chemical*. Vol.184, pp.361–370.

Martin, R.R.L., Neves, M., Silvestre, A.J.D., Silvia, A.M.S.J., Caveleiro, J.A.S. 1999. "Oxidation of Aromatic Monoterpenes with Hydrogen Peroxide Catalyzed by Mn Porpyrin Complexes", *Journal of Molecular Catalysis A*: *Chemical*. Vol.137, pp. 41-47.

Martin, R.R.L., Neves, G. 2001. "Oxidation of Unsaturated Monoterpenes with Hydrogen Peroxide Catalysed by Manganase (III) Porphyrin Complexes". *Journal of Molecular Catalysis A*: *Chemical*. Vol.172, pp.33-42.

Maurya, M.R., Titinchi, S.J.J., Chand, S., Mishra, I.M. 2002. "Zeolite-Encapsulated Cr(III), Fe(III), Ni(II), Zn(II) and Bi(III) Salpn Complexes as Catalysts for the Decomposition of H_2O_2 and Oxidation of Phenol.", *Journal of Moleculer Catalysis A*: *Chemical*. Vol.180, pp.201-209.

Maurya, M.R., Titinchi, S.J.J., Chand, S. 2002. "Spectroscopic and Catalytic Activity Study of *N*,*N*-bis(salicylidene)propane-1,3-diamine Copper(II) Encapsulated in Zeolite-Y", *Applied Catalysis A*: *General*. Vol.228, pp.177-187.

Maurya, M.R., Jain, I., Titinchi, S.J.J. 2003. "Coordination Polymers Based on Bridging Methylene Group as Catalysts for the Liquid Phase Hydroxylation of Phenol", *Applied Catalysis A*: *General*. Vol.249, pp.139-149.

Milos, M., Mastelic, J., Jerkovic, I. 2000. "Chemical Composition and Antioxidant Effect of Glycosidically Bound Volatile Compounds from Oregano (Origanum Vulgare L. Ssp. Hirtum)"**,** *Food Chemistry*. Vol.71, pp.79-83.

Milos, M.A. 2001. "A Comparative Study of Biomimetic Oxidation of Oregano Essential Oil by H_2O_2 or $KHSO_5$ Catalyzed by Fe(III) Meso-tetraphenylporphyrin or Fe(III) Phthalocyianine", *Applied Catalysis A*: *General*. Vol.216, pp.157-161.

Monteiro, J.L.F., Veloso, C.O. 2004. "Catalytic Conversion of Terpenes into Fine Chemicals", *Topics in Catalysis*.Vol.27, pp.1-4.

Morrison, B., 1992. *Organic Chemistry*, (New York University, New Jersey).

Nakagaki, S., Xavier, C.R., Wosniak, A., Mangrich, A., Wypch, F., Cantao, M.P.,Denicolo, I., Kubota, L.T. 2000. "Synthesis and Characterization of Zeolite-Encapsulated Metalloporphyrins", *A*: *Physicochemical and Engineering Aspects*. Vol. 168, pp. 261-276.

Ramesh, R., Suganthy, P.K., Natarajan, K. 1996. "Synthesis, Spectra and Electrochemistry of Ru (III) Complexes with Tetradentate Schiff Bases", *Synthesis and Reactivity in Inorganic and Metal-Organic Chemistry*. Vol.26 (1), pp.47-60.

Richardson, J.T., 1989. *Principles of Catalyst Development*, (University of Houston, Texas), pp. 35-79.

Rosa, X.I.L., Viana, C.M.C.P., Manso, O.A. 2000. "Biomimetical Catalytic Activity of Iron III Porphyrins Encapsulated in the Zeolite", *Journal of Molecular Catalysis A*: *Chemical*. Vol. 160, pp.199–208.

Salem, I.A., Maazawi, M.E., Zaki, A., 2000. *Kinetics and Mechanisms of Decomposition Reaction of Hydrogen Peroxide in Presence of Metal Complexes*, (John Wiley and Sons, New York), pp. 643-666.

Sanderson, W.R. 2000. “Cleaner Industrial Processes Using Hydrogen Peroxide”, *Pure Applied Chemistry*. Vol. 72, No. 7, pp.1289-1304.

Santos, I.C.M.S., Simões, M.M.Q., Pereira, M.M.M.S., Martin, R.R.L., Neves, M.G.P.M.S., Silvestre, A.J.D., Cavaleiro, J.A.S., Cavaleiro, A.M.V. 2003. “Oxidation of Monoterpenes with Hydrogen Peroxide Catalysed by Keggin Type Tungstoborates”, *Journal of Moleculer Catalysis A*: *Chemical*. Vol.195, pp.253-262.

Satterfield, C. N., 1991. *Heterogeneous Catalysis in Industrial Practice*, (McGraw-Hill, New York).

Sen, S.E., Smith, S.M, Sullivan, K.A. 1999. “Organic Transformation using Zeolites and Zeotype Materials”, *Tetrahedron*. Vol. 55, pp.12657-12698.

Sheldon, R.A., Arends, I.W.C.E., Lempers, H.E.B. 1998. “Liquid Phase Oxidation at Metal Ions and Complexes in Constrained Environments”, *Catalysis Today*. Vol. 41, pp. 387-407.

Shevade, S.S., Raja, R., Kotasthane, A.N. 1999. “Copper(II) Phthalocyanines Entrapped in MFI Zeolite Catalysts and Their Application in Phenol Hydroxylation”, *Applied Catalysis General*: *A*. Vol. 178, pp.243-249.

Sinfelt, J.H. 2002. “Role of Surface Science in Catalysis”, *Surface Science*. Vol. 500, pp.923-946.

Skrobot, F.C., Valente, A., Neves, G., Rosa, I., Rocha, J., Cavaleiro, J.A.S. 2003. “Monoterpenes Oxidation in the Presence of Y Zeolite-Entrapped Manganese(III) Tetra(4-*N*-benzylpyridyl) Porphyrin”, *Journal of Molecular Catalysis A*: *Chemical*. Vol. 201, pp.211-222.

Solomons, T.W.G., 1988. *Organic Chemistry,* (John Wiley and Sons, South Florida).

Varkey , S.P., Ratnasamy, C., Ratnasamy, P. 1998. “Zeolite-Encapsulated Manganese III Salen Complexes ”, *Journal of Molecular Catalysis A*: *Chemical*. Vol. 135, pp.295-306.

Velde, F.V.D., Arends, I.W.C.E., Sheldon, R.A. 2000. “Biocatalytic and Biomimetic Oxidations with Vanadium”, *Journal of Inorganic Biochemistry*. Vol. 80, pp. 81-89.

Weitkamp, J., 1999. *Catalysis and Zeolites, Fundamentals and Applications,* (Springer-Verlag, Berlin), pp. 1-5.

Xavier, K.O., Chacko, J., Mohammed Yusuff, K.K. 2004. “Zeolite Encapsulated Co(II), Ni(II) and Cu(II) Complexes as Catalysts for Partial Oxidation of Benzyl Alcohol and Ethylbenzene ”, *Applied Catalysis A*: *General*. Vol. *258*, pp.251-259.

APPENDIX A

DETERMINATION OF HYDROGEN PEROXIDE CONCENTRATION

This method describes the determination of hydrogen peroxide concentration in an aqueous solution. The chemical background is the reaction of potassium permanganate with hydrogen peroxide in acidic medium according to the following equation:

$2\ KMnO_4 + 5\ H_2O_2 + 4\ H_2SO_4 \rightarrow 2\ KHSO_4 + 2\ MnSO_4 + 8\ H_2O + 5\ O_2$

The procedure can be carried out when using titration equipment

An exactly weighed sample of the H_2O_2 containing solution is added to 50 ml 2.5 M sulphuric acid in a flask. The sample is titrated with 0.02 M standard potassium permanganate solution while mixing vigorously. By using manual titration, titrate until a pale pink coloration persists for a while. The content of hydrogen peroxide in the solution is calculated from the consumption of $KMNO_4$ as seen below.

H_2O_2 in solution (mol/ml) = 0.02 (mol/lt) $KMnO_4$ x consumed $KMnO_4$ (ml) x (5/2)

APPENDIX B

CALIBRATION CURVES

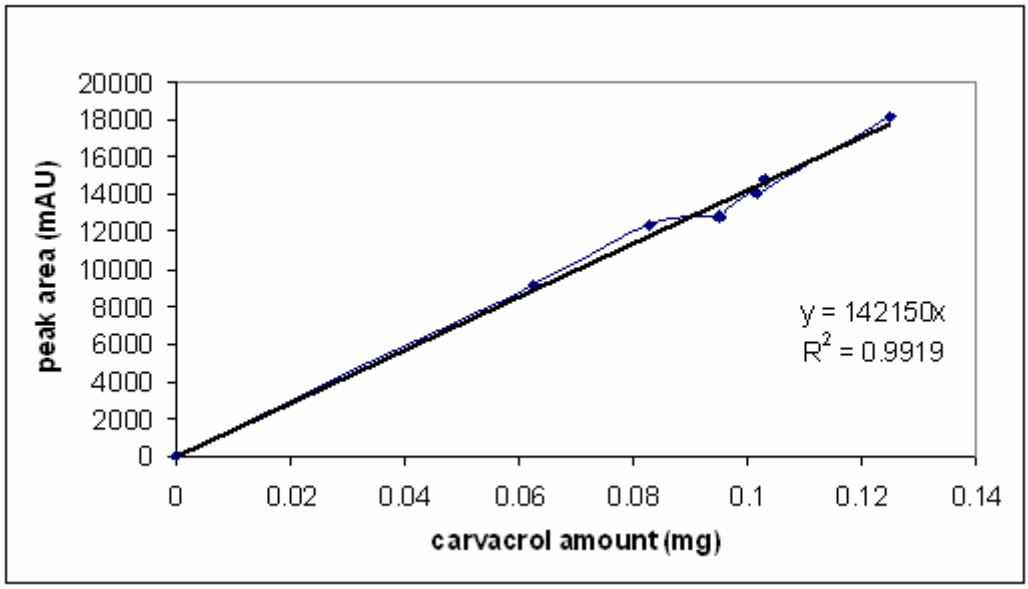

Figure B.1. Calibration curve of carvacrol

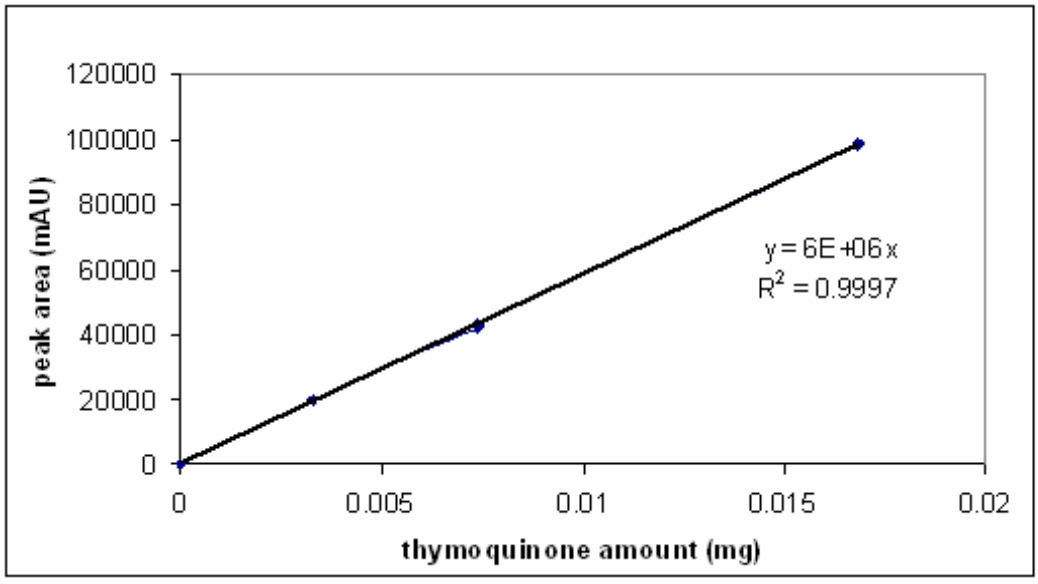

Figure B.2. Calibration curve of thymoquinone